

Accelerator operation report

S.Reimann¹, A.Bloch-Sp  th¹, P. Sch  tt¹, M. Sapinski¹, O.Geithner¹
¹GSI, Darmstadt, Germany

This report describes the operation statistics of the GSI accelerator facility of the year 2016. The information is based on the data of the new GSI electronic log-book OLOG [1], which allows a detailed evaluation of operation statistics especially for the time-sharing operation mode of the GSI accelerators.

General Overview

After a 4.5-month long shutdown and maintenance period, the re-commissioning of the UNILAC started in April. From end of April till July, a single beam time block was scheduled and in comparison to the previous year, the GSI accelerator facility was completely operational again with one exception. Since the UNILAC RF-System is under construction, the maximum energy of the Alvarez section was defined to 5.89 MeV/u. So the synchrotron had to be operated with higher RF-harmonic number, what in the end was limiting the maximum revolution frequency and therefore the SIS18 extraction energy.

In total the UNILAC has been in operation for 2448 hours and the SIS18 for 1776 hours (504 hours are included for the commissioning of each accelerator after shutdown).

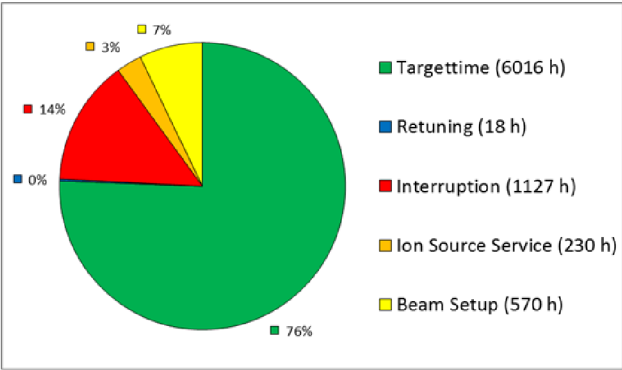


Figure 1: Distribution of overall beam time for all beam modes and experiments (parallel operation, no standby).

Figure 1 shows the overall beam time of the whole facility with respect to the parallel operation modes. In total 6016 hours of beam-on-target-time were successfully delivered to the different experiments, which is 76% of total beam time (the same as in 2015).

The percentage of interruption time increased drastically from 8% in 2015 to 14%. Fortunately this loss was completely compensated by a decreasing time for setup and retuning. Main reason was the very efficient beam time schedule which was developed in close cooperation of the experiments with the accelerator division under consideration of the limitations of the machines and the personnel situation. The dedicated hands-on operator

training shifts [2], which we established this year at GSI, may also have had influence on this improvement.

Since the SIS18 was not operated in 2015, Table 1 shows also the beam time statistics of 2014, when SIS18 was last time fully operational. In comparison to the 2014 beam time both, percentage of setup- and interruption times, could be reduced this year.

Table 1: Overall beam time of the GSI accelerator facility

	2014	2015	2016
Integral target time	12000 h	5000 h	6016 h
	70%	76%	76%
Setup & Retuning	2300 h	873 h	588 h
	13%	13%	7%
Ion Source Service	514 h	218 h	230 h
	3%	3%	3%
Time for interruption	2391 h	533 h	1127 h
	14%	8%	14%
Total beam time	17133 h	6624 h	7960 h

Experiments

Figure 2 gives an overview of target time for different experimental areas. The fraction of the beam branches of the UNILAC are marked in blue, the ESR in green and the different experimental caves behind the SIS are displayed as orange slices. Details corresponding to the different experimental programs are given in [3].

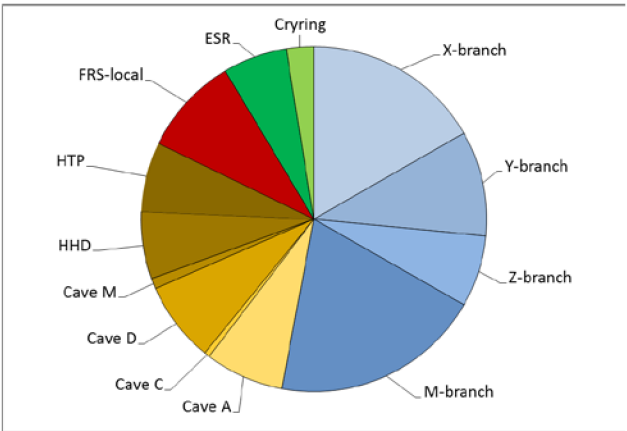


Figure 2: Distribution of target time to the different experimental areas.

Over the year, the UNILAC delivered beams to 29 different experiments. Main user was the Material Science at the M-branch. In addition 25 fixed target experiments for FAIR detector tests have been performed behind the SIS18 and at the ESR internal target. Besides, the transfer line from the ESR to the CRYRING has been commissioned during this beam time.

Breakdown Statistics

Table 4 shows all unscheduled down time events in more detail. Problems with the RF-System and structures (especially UNILAC) are dominating this statistics again and are now responsible for 56% of overall downtime. The UNILAC RF-Transmitter-System is replaced at the moment and is expected to be fully operational again in beam time 2018. Nevertheless the replacement of the post stripper section is a necessary long term task to be done.

Table 4: Sum of all unscheduled down time events per category (parallel operation is not taken into account)

	Duration	No. of events
Power Supplies	200 h	112
Vacuum and RF-Structures	154 h	49
Beam Instrumentation	70 h	10
Operation	3 h	4
Safety-/ Interlock System	73 h	14
Ion Sources	21 h	31
RF-System	382 h	146
Controls	9 h	9
Infrastructure	26 h	6
Others / Ambiguous	10 h	17
Total	948 h	398

Isotope Statistic

During 2016, 11 different isotopes have been accelerated from 6 different ion sources.

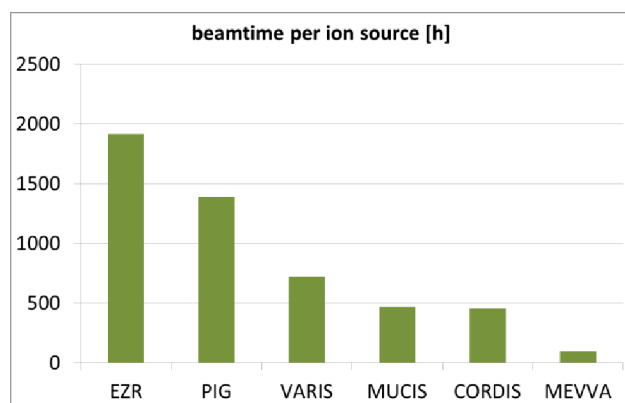


Figure 3: Distribution of integral beam time per ion source.

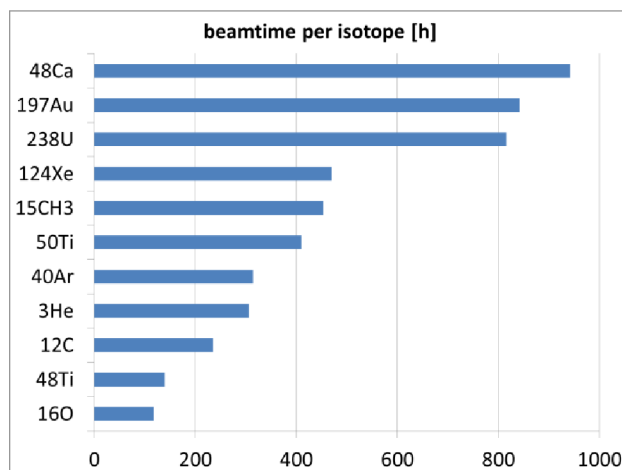


Figure 4: Distribution of integral beam time per isotope.

Figure 3 shows the distribution of the beam time per ion source and figure 4 shows the distribution of the integral beam time (parallel operation) per isotope. Calcium (from ECR), Gold (from PIG) and Uranium (from VARIS) are dominating both statistics.

Summary

Even though half of the Alvarez-Section was not operational this year and the SIS18 has been operated in an unusual mode, the beam time was a success for both the accelerator division and the experiments. The limitation of the parallel operation modes at the SIS18 to few elements and the close cooperation with the experiment speakers helped, to completely process the ambitious beam time schedule.

Outlook

For 2017 no beam time is scheduled as the site construction project GAF (German, GSI Connection to FAIR) forces GSI accelerators into a 2 years shutdown period. Within this shutdown many maintenance and upgrade measures on all accelerators will be performed.

Until next beam time in 2018 the main control room has to be refurbished and upgraded, to fit the needs of the new operation software and control system which is planned to be installed during the controls retrofitting project next year. In addition it is planned, to go first steps into automation and digitalization.

We are also working on a new way to analyse and present statistical data on machines operation, which will help to have a more complete picture of the availability of the GSI accelerator complex.

References

- [1] P. Schuett, the GSI Operation Logbook OLog, WAO 7th, Seoul, Korea, 2010
- [2] M. Vossberg and S. Reimann, Operator Training Shift Experience, WAO 10th, China, Shanghai, 2016
- [3] Report of beam time coordinator, this report

Shutdown report

P.Schütt, M.Vossberg, S.Reimann
GSI, Darmstadt, Germany

This report describes the main service and upgrade measures of the GSI accelerator facilities, which were started in 2016 and will be continued until mid-2018. The presented information is based on the work of the shutdown coordination and the corresponding MS-Project shutdown schedules.

General Overview

In July 2016 began the longest shutdown GSI has ever seen. It is expected to end in May 2018. The planning started well in advance [1] with a collection of the major tasks planned by the respective machine coordinators. The most important projects have been fit into a common time line (see Figure 1). It is derived from a detailed MS-Project schedule comprising more than 1500 individual tasks. This way, conflicts were identified and the individual schedules were synchronized. Weekly meetings are organized with the machine coordinators and representatives of all involved departments, including civil construction and infrastructure. There, the actual progress is monitored, pending work and critical incidents are discussed and the overall schedule is adapted accordingly.

Work Packages

The largest work package is the civil construction project GAF (GSI Anbindung an FAIR, Link of GSI to FAIR), which comprises additional shielding of SIS18, fire protection measures, as well as the connection of the new beam line tunnel towards FAIR to the existing TR hall (s. Figure 2). The GAF project implies that SIS accelerator components are inaccessible during most of the construction work. Therefore, maintenance and repair work on the kicker and on RF cavities was scheduled at the beginning of the shutdown and was finished, before the start of GAF. The largest project at the UNILAC is the modernization of post-stripper RF systems, which started in 2015. It needs regular test periods with full infrastructure available. This is in conflict with the refurbishment of the Heating, Ventilation and Air Conditioning (HVAC) system of the UNILAC tunnel. Careful coordination of these projects is mandatory to finish in time for the beam time 2018. Ion source development requires several test periods. The electrostatic acceleration section of terminal north will be renewed.

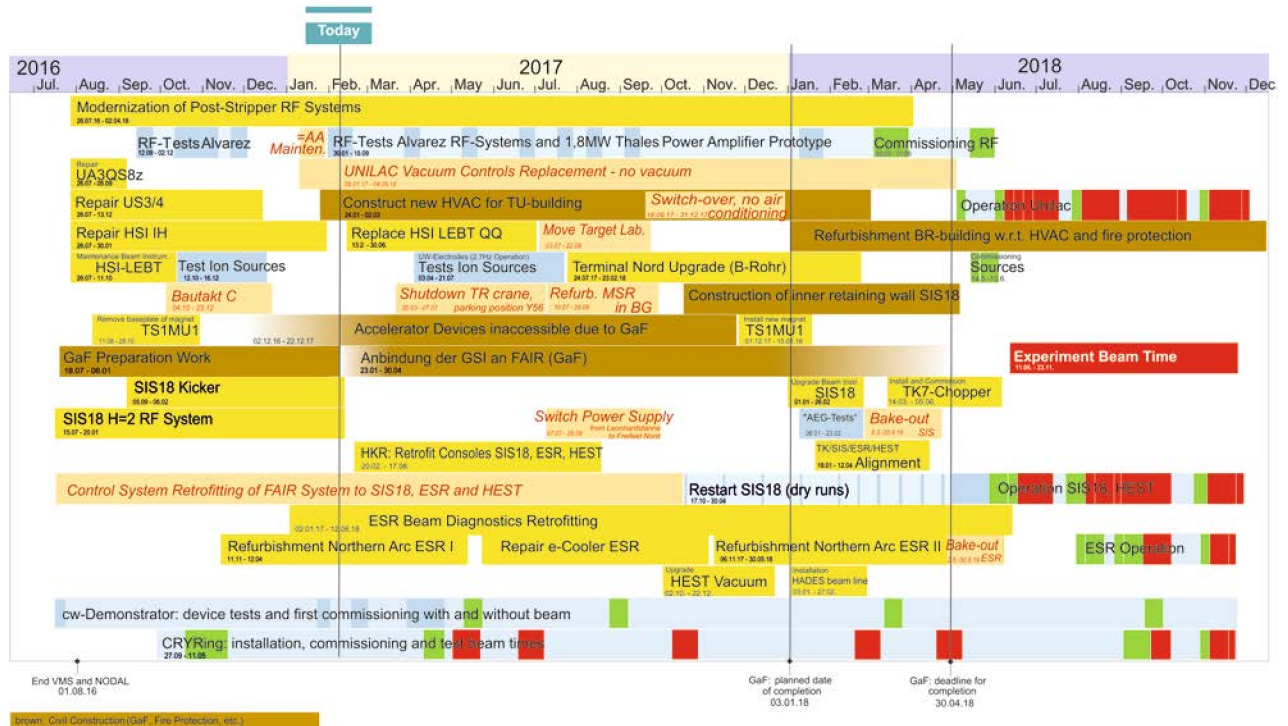


Figure 1: Timeline of the long Shutdown 2016-2018, status February 2017.



Another important project is the retrofitting of the FAIR control system to SIS18, ESR and HEST: the previous control system was finally shut down after the beam time 2016. In order to ensure smooth commissioning of the new control system, dry runs are scheduled half a year before the next beam time. These interfere with the GAF project. The control system refurbishment also implies beam diagnostics upgrades and the implementation of modern consoles for SIS18 and ESR in the main control room. These consoles shall have the same layout as the planned consoles for FAIR.

ESR requires a vacuum refurbishment of the northern arc, following the respective work on the southern arc in the last shutdown 2015. Repair of a short-circuit fault in the electron cooler of the ESR will need several months, for this work the cooler must be almost completely dismantled.

The shutdown work in the HEST concentrates on the upgrade of the HADES beam line with respect to the aperture and beam diagnostics and the refurbishment of some vacuum components.

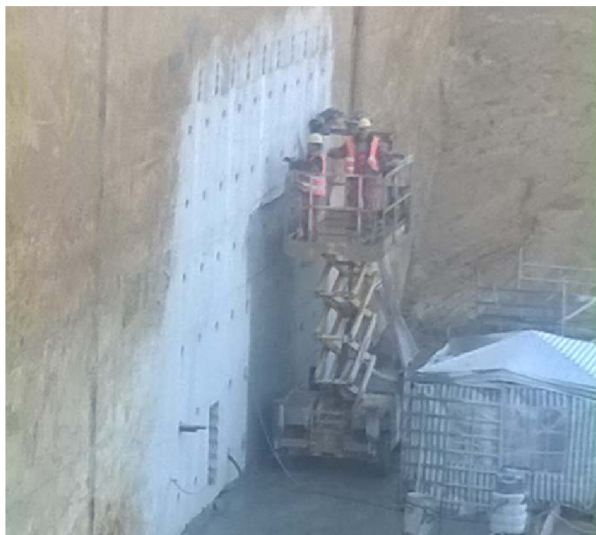


Figure 2: Construction Area of GAF: wall of existing hall is opened to connect new beam line tunnel towards FAIR.

The pulsed power connection for the main magnets of SIS18 and ESR will be switched from Leonhardstanne to “Freifeld Nord” in FAIR. Afterwards, the SAT of the new power supplies needs to be performed.

Due to civil construction not only in GAF but also for the new FAIR buildings, the accelerator tunnel floors will move and the corresponding accelerators components accordingly. Therefore, a thorough survey is scheduled and alignment will be necessary.

Development of the cw-demonstrator is on-going. The power coupler is delivered and the amplifier is ready. First tests with beam will take place end of June.

CRYRing was set up and adjusted, first tests took place in December 2016 and commissioning with beam is planned until 2018.

Critical Path

The end of the beam time 2016 was determined by the need to prepare for the GAF civil construction project. The deadline for this project is April 2018, with all work inside the accelerator tunnels finished in January 2018, in order to enable timely recommissioning for the beam time 2018.

Other projects with long duration are:

- modernization of post-stripper RF systems
- UNILAC vacuum controls replacement
- refurbishment of HVAC of the UNILAC tunnel
- retrofitting of the FAIR control system

Status and Outlook

At the end of 2016, SIS18 and HEST were prepared for GAF. The actual construction work was delayed by several weeks which could be used for completion of work on kicker and RF systems, which had originally been planned for 2018.

UNILAC vacuum controls replacement had to be postponed to the next shutdown because of shortage of manpower: with the available workforce, the project could not be started early enough to be finished before the scheduled beam time 2018.

Not all proposed projects can be fully supported during this shutdown for reasons of capacity. This includes e.g.

- replacement of the UNILAC personal safety system TVS (windows NT based server)
- refurbishment of the chopper in front of injection into SIS18
- ionization profile monitors (IPM) for SIS and ESR
- vacuum upgrade measures in the HEST
- upgrade of beam line FRS to ESR
- upgrade of HADES beamline
- preparation of beam line and cave C for Mini CBM
- upgrade of FRS

For a timely completion of these tasks, a decision in the first quarter of 2017 is mandatory.

Due to personal shortage in all involved departments and high priority tasks for the FAIR project, the progress in many tasks is slower than expected. Nevertheless, a timely completion for the beam time 2018 is still feasible.

References

- [1] S. Reimann, P. Schütt, Scheduling and Tracing of Maintenance Tasks in Long Shutdowns, ARW 5th, Knoxville, Tennessee, USA, 2015

R&D Status of the new CH cavities for the sc cw Heavy Ion LINAC@GSI

M. Basten^{#,1}, K. Aulenbacher^{3,4}, W. Barth^{2,3}, M. Busch¹, F. Dziuba^{1,3}, V. Gettmann³, M. Heilmann², M. Miski-Oglu³, H. Podlech¹, M. Schwarz¹, S. Yaramyshev²

¹Goethe University, 60438 Frankfurt am Main, Germany; ²GSI Helmholtzzentrum, 64291 Darmstadt, Germany;

³Helmholtz-Institut Mainz (HIM), 55099 Mainz, Germany; ⁴KPH Mainz University, 55128 Mainz, Germany

Presently cavity 2 and 3 of the advanced cw linac demonstrator at GSI is under construction at Research Instruments (RI). After the successful beam test of the demonstrator at GSI-HLI in 2017 this is the next milestone realizing a new sc heavy ion cw-LINAC at GSI. The demonstrator cavity had been successfully rf tested at cryo conditions at Frankfurt University [1] and GSI [2]. The recent design of the sc cw-LINAC comprises the demonstrator and cavity 2 and 3 as first cryomodule and up to 4 additional cryomodules each equipped with three short CH-cavities. The overall design of this standard cryomodule will be used for all following cavities. The recent short cavity with 8 accelerating cells is designed for high power applications at a design gradient of 5 MV/m. Its resonant frequency is the second harmonic of the High Charge Injector (HLI) at GSI, Darmstadt. Table 1 shows the main parameters of the short sc 217 MHz CH-cavity. In Figure 1 the layout of this cavity is depicted.

Design of the short CH-Cavity

The design of the cavity is based on 8 equidistant gaps without girders and with stiffening brackets at the front and end cap to reduce pressure sensitivity. Avoiding high fabrication costs and extended fabrication duration the short cavity design is without girders. In a final step the design has been changed to provide for constant welding depths at the stems. As a consequence the cavity is flattened around the stems. Also the design of the bellow tuner was changed to reduce mechanical stress and the number of parallel segments.

Parameter	Unit	
β		0.069
Frequency	MHz	216,816
Accelerating cells		8
Length ($\beta\lambda$ -definition)	mm	381.6
Cavity diameter (outer)	mm	400
Cell length	mm	47.7
Aperture diameter	mm	30
Static tuner		3
Dynamic bellow tuner		2
Wall thickness	mm	3-4
Accelerating gradient	MV/m	5
E_p/E_a		5.2
B_p/E_a	mT/(MV/m)	<10
G	Ω	50
R_a/Q_0		1070

Table 1: Specifications of the 217 MHz short CH-cavity



Figure 1: Final design of the sc 217 MHz CH-cavity.

Status

The final design of the 217 MHz short CH-cavity was finished at the beginning of 2015; the construction started end of 2015. Several simulations with CST-Microwave-Studio [3], as well as ANSYS Workbench [4] have been performed to determine crucial parameters and eigenfrequencies. The niobium raw material was delivered to RI company at the end of 2015. The construction phase was scheduled till 2017. Recently RI faces several difficulties concerning the flattened parts around the stems. Problems during the mechanical process of pressing the cylindrical cavity have to be solved. The center of the flattened parts reach 0.4 mm out of in the cavity while the edges are facing 0.7 mm inside the cavity. RI has to correct these parts assuring for alignment of all stems after the welding process. First frequency measurements are already performed confirming consistent results between measurements and simulations.

References

- [1] F. Dziuba et al., First Performance Test on the Superconducting 217 MHz CH Cavity at 4 K, LINAC 2016, East Lansing, USA, THPLR033
- [2] F. Dziuba et al., First cold tests of the superconducting cw demonstrator at GSI, RuPAC2016, St. Petersburg, Russia, WECBMH01
- [3] CST Microwave Studio; <http://www.cst.com>
- [4] ANSYS, Inc.; www.ansys.com

[#]Basten@iap.uni-frankfurt.de

Horizontal RF tests of the superconducting 217 MHz CH cavity for the HIM/GSI-cw LINAC

F. Dziuba^{*1,2}, *M. Amberg*^{1,3}, *K. Aulenbacher*^{1,4}, *W. Barth*^{1,2,5}, *M. Basten*³, *M. Busch*³, *V. Gettmann*¹, *M. Heilmann*², *M. Miski-Oglu*¹, *H. Podlech*³, *J. Salvatore*², *A. Schnase*², *M. Schwarz*³, and *S. Yarymyshev*^{2,5}

¹HIM, Mainz, Germany; ²GSI, Darmstadt, Germany; ³IAP, Frankfurt, Germany; ⁴KPH, Mainz, Germany; ⁵MEPhI, Moscow, Russia

Introduction

The continuous wave (cw) demonstrator is the first prototype of a new superconducting (sc) cw linac, which is proposed to keep the Super Heavy Element (SHE) research program at GSI competitive. The demonstrator consists of a sc 217 MHz crossbar-H-mode (CH) multigap cavity embedded by two sc 9.3 T solenoids mounted in a horizontal cryomodule. At the end of 2016 the rf performance of the cavity has been extensively tested at 4.2 K with low level rf power.

Measurement results

A first rf test of the sc 217 MHz CH cavity (without helium vessel) at the Institute of Applied Physics (IAP) of Goethe University Frankfurt has been performed beginning of 2016 [1]. At that time the performance of the cavity was limited by field emission caused by insufficient surface preparation. Nevertheless, a maximum accelerating gradient of $E_a = 6.9$ MV/m at $Q_0 = 2.19 \cdot 10^8$ was reached (see Figure 1).

After the final assembly of the helium vessel and further High Pressure Rinsing (HPR) preparation, the cavity was delivered to GSI and prepared for a second rf test in a horizontal cryomodule (see Figure 2) [2]. A 50 W broadband amplifier was used to deliver the required rf power. The cavity runs as a generator driven resonator directed by an rf control system. Further equipment, namely a network analyzer, three power meters and a scope has been used for rf measurements. Initially, the cavity has been passively precooled down to 218 K by the N_2 shield of the cryostat. Hereafter, the temperature was quickly lowered (3 K/min in average) applied by liquid helium to 4.2 K avoiding hydrogen related Q -disease. Subsequently, rf conditioning has been performed. All multipacting barriers up to 4 MV/m could be surmounted permanently. In a next step the rf performance of the cavity was reviewed. Figure 1 shows the related Q_0 vs. E_a curves measured in vertical position (without helium vessel, red curve) and in horizontal orientation (with helium vessel, blue curve), respectively. The maximum Q -value at a low field level (Q_0^{low}) was measured as $1.37 \cdot 10^9$. Recently, the cavity showed an improved performance due to an advanced HPR treatment. The initial

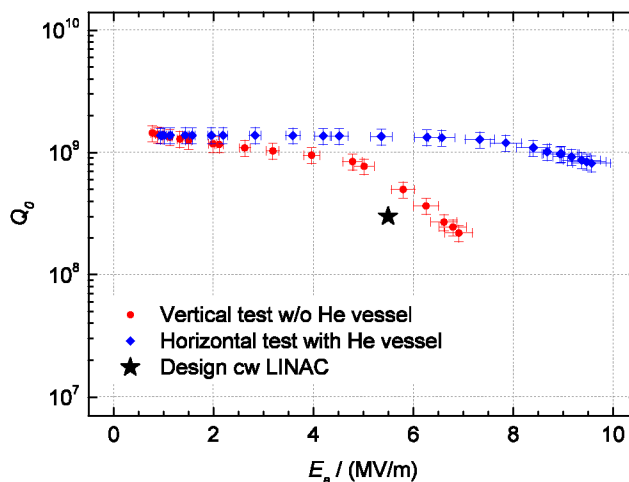


Figure 1: Q_0 vs. E_a curves at 4.2 K [2].



Figure 2: Superconducting 217 MHz CH cavity during manufacturing (left) and finally mounted into the support frame of the horizontal cryomodule (right) [2].

design quality factor at 5.5 MV/m has been exceeded by a factor of 4. Furthermore, a maximum accelerating gradient of $E_a = 9.6$ MV/m at $Q_0 = 8.14 \cdot 10^8$ was reached, which increases the cw linac capabilities in terms of operation with heavy ions as well of higher beam energies.

References

- [1] F. Dziuba et al., in Proc. of LINAC2016, East Lansing, Michigan, USA, THPLR044, 2016, (to be published).
- [2] F. Dziuba, “First Cold Tests of the Superconducting CW Demonstrator at GSI”, RuPac’16, St. Petersburg, Russia, November 2016, p. 83–85

* f.dziuba@gsi.de

Preparation work at the 325 MHz test stand at GSI for Klystron FAT and SAT

A. Schnase, M. Helmecke, E. Plechov, S. Pütz, G. Schreiber
GSI, Darmstadt, Germany

In 2016 the 325 MHz test stand was used to continue high power testing [1] of a CH prototype cavity for the FAIR proton Linac. Finally up to 2.7 MW forward power were delivered to find out the limits and to condition this CH cavity [2]. It was confirmed that the whole high power signal chain from klystron via circulator to the cavity coupler works as expected. This klystron system was also used to evaluate the RF power limits of a prototype 325 MHz ladder-RFQ [3]. Here up to 487 kW of forward power could be sent to the cavity.

Short afterwards the Klystron HV modulator, which was a loan from CERN Linac 4, had to be returned. In order to restart Klystron operation in 2018 the design process for Klystron modulators for the pLinac was started [4]. The 45 kW buncher amplifiers are prepared to be connected to the CH prototype cavity to check the result of remodeling work and to conduct the related SAT.

The test stand will be used for cavity testing and conditioning, and also for SAT (Site Acceptance Test) of RF transmission line components as:

Circulators, rectangular waveguides, coaxial RF power transmission lines, transitions from WR 2300 waveguide to coaxial and high power loads. Of equal importance are tests of HV modulators, Klystrons and LLRF systems.

Two In-Kind contracts between GSI/FAIR and the laboratory CNRS were prepared. One contract covers RF components used at the test stand. The other covers the series production of Thales TH 2181 klystrons, which after delivery to GSI/FAIR need to be tested (SAT) before installation to the pLinac klystron gallery.

Directional coupler remodeling work

For the FAT (Factory Acceptance Test) of the TH 2181 klystrons at Thales, the RF power is measured with directional couplers. We already noticed that their directivity was below requirements and developed an external cure [5]. The 4 dual directional couplers for the test stand and the 7 dual directional couplers for the pLinac itself contain different versions of loop couplers as shown in fig. 1. The geometry on the left provides directivity not better than 23 dB. The geometry in the center provides a better directivity in the range of 30 dB.

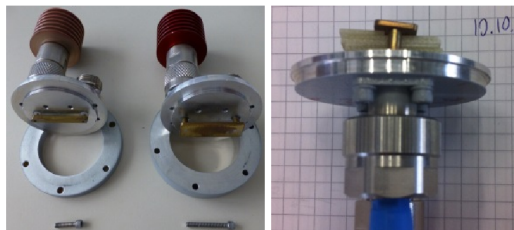


Figure 1: Different coupling loop geometries.

The measured reflection S_{11} on the Type N port was only in the order of -20 dB. Calculations show that the ge-

ometry behaves like a PCB stripline that matches to 50 Ω , when filled with FR4 circuit board material. With the loop filled with FR4 (right geometry in Fig. 1), and a selected precise termination, S_{11} improves to -40...-50 dB. This modified loop leads to an improved directivity in the order of 40...50 dB. The modifications before (left) and after (right) are shown in Fig. 2 for the dual coupler serial #1119-987. The directivity improves from 22 to 42 dB.



Figure 2: Modification process for coupler #1119-987.

These modifications were applied to all 4 dual directional couplers of series #1119. The results (before / after upgrade) are displayed in figure 3. Two of these modified dual couplers were handed to Thales for next FATs.

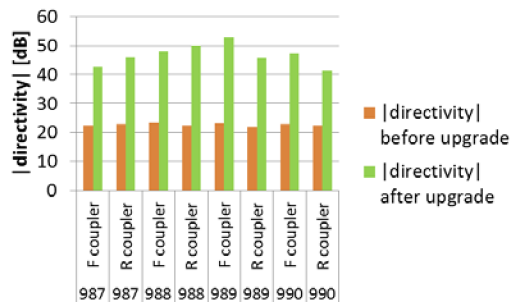


Figure 3: Comparison of improved directivity.

Outlook

Next 7 dual direction couplers and 7 6-port couplers will be upgraded. This requires machined FR4 inserts and a calibration procedure, improved by driving the movable short with an embedded system controlled stepper motor.

References

- [1] A. Schnase, et. al. "Progress of the 325 MHz Test Stand at GSI in 2015", GSI sci. report 2015, p. 340
- [2] G. Schreiber, et. al., "First High Power Tests at the 325 MHz RF Test Stand at GSI", Proc. 28th Linear Acc. Conf. (LINAC'16), East-Lansing, MI, USA, Sep. 2016, MOPLR067, pp. 273-275
- [3] M. Schütt, et. al., "Development and Measurements of a 325 MHz RFQ", Proc. 28th Linear Acc. Conf. (LINAC'16), Sep. 2016, TUPLR053, pp. 543-545
- [4] S. Pütz, A. Schnase, G. Schreiber "Design and Production of Klystron Modulators for the pLINAC", this scientific report
- [5] A. Schnase, E. Plechov, G. Schreiber "Development of a procedure for directional coupler calibration at the 325 MHz test stand, GSI sci. report 2015, p. 341

New simulation code for ionization profile monitors

D. Vilsmeier^{*1,2}, *P. Forck*¹, and *M. Sapinski*¹

¹GSI, Darmstadt, Germany; ²Universität Regensburg, Germany

Ionization Profile Monitors (IPMs) are devices for non-invasive beam profile measurement. They make use of phenomena of rest gas ionization by the beam. Electrons or ions produced in the ionization process are extracted from the region of interaction between the beam and the rest gas, and transported, using external electric and magnetic fields (called guiding fields), towards a detection device. The detection device is usually based on a phosphor screen or a segmented anode. The distribution of the positions of electrons or ions on the detector allow for reconstruction of the beam profile.

Although the principle of the IPM operation is simple, the reconstructed beam profile can be distorted due to various effects. Those effects include the nonuniformities of the guiding fields, initial kick given to electrons during the ionization (initial velocities) or the influence of the bunch fields on the trajectories of particles. Most of those effects cannot be treated analytically and specialized simulation program is needed. Such a program typically incorporates particle generation in the ionization process, calculation of the beam fields and tracking of charged particles in a superposition of transient bunch fields and constant guiding fields.

Surprisingly, none of the investigated available codes (CST and Geant4) has an ability to perform this kind of simulations therefore, in almost every laboratory which uses IPMs, researchers wrote their own codes [1,2]. Those codes are tuned to particular needs of the laboratories and are usually designed for specific cases only. Nevertheless, they contain a lot of common aspects.

In this situation we decided to create a modern, universal simulation code [3], which is easy to set up and which contains algorithms adequate for most of the investigated IPMs. The program, written in Python, has a modular structure and is easily extendable (it is being extended to Beam Induced Fluorescence monitor case). The main components are: ionization, guiding fields, bunch fields and tracking. Currently those components contain the following methods:

- Ionization: zero velocities, Voigt analytical formula [4] and phenomenological parametrization of double differential cross-section. This component is an independent package, so it can be used by other projects.
- Guiding fields: uniform fields and CST field map.
- Bunch field: analytical expression for special cases

(Basetti-Erskine, etc.) and numerical Poisson solvers (2D, 3D).

- Tracking: Runge-Kutta method, Boris algorithm and analytical expression (for parallel electric and magnetic fields only).

Additional components describe the detector part, the rest gas properties and manage the simulation output. The Graphical User Interface to the simulation program is written using Qt libraries and the simulation configuration, as well as the simulation output, can be handled using XML format. The code is open source and accessible via Python Package Index (virtual-ipm package).

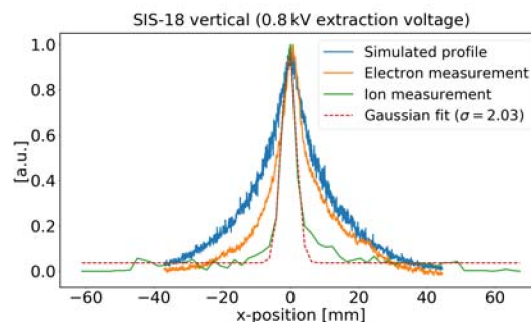


Figure 1: Measurement and simulation results for SIS18 IPM: measured beam profile (green), simulated beam profile distorted by the initial velocities of electrons and bunch field (blue) and the corresponding measurement (orange).

Figure 1 presents an example of results of the simulation program. The data were measured on June 28th, 2016 during $^{124}\text{Xe}^{43+}$ beam time using vertical IPM in SIS-18. The device was working in electron collection mode and the extraction voltage was decreased from 4 kV to 800 V in order to investigate the profile distortion. The beam had asymmetric shape, what has not been taken into account by the simulation, therefore a good agreement is seen only for half of the profile.

References

- [1] M. Sapinski et al., "Ionization Profile Monitor Simulations - Status and Future Plans", IBIC 2016, Barcelona, September 2016, TUPG71
- [2] <https://twiki.cern.ch/twiki/bin/view/IPMSim>
- [3] <https://gitlab.com/IPMSim/Virtual-IPM/>
- [4] A. Voikov et al., J.Phys.B: At.Mol.Opt.Phys.**32**(1999) p. 3923

* d.vilsmeier@gsi.de

BIF profile monitor development for electron lenses

S. Udrea¹, P. Forck¹, E. Barrios Diaz², N. Chritin², O. R. Jones², P. Magagnin², G. Schneider²,
R. Veness², V. Tzoganis³, C. Welsch³, H. Zhang³

¹GSI, Darmstadt, Germany; ²CERN, Geneva, Switzerland; ³Cockcroft Institute, Warrington, UK

Electron lenses (e-lens) [1] have been proposed and used to mitigate several issues related to the beam dynamics in high current synchrotrons. As part of the collimation upgrade for the high luminosity upgrade of LHC a hollow electron lens system is presently under development. Moreover, at GSI an electron lens system also is proposed for space charge compensation in the SIS-18 synchrotron to decrease the tune spread and allow for the high intensities at the future FAIR facility. To ensure for a precise alignment between the ion beam and the low energy electron beam a transverse profile monitor based on an intersecting gas sheet and the observation of beam induced fluorescence (BIF) is under development within a collaboration between CERN, Cockcroft Institute and GSI [2], as schematically shown in Fig. 1.

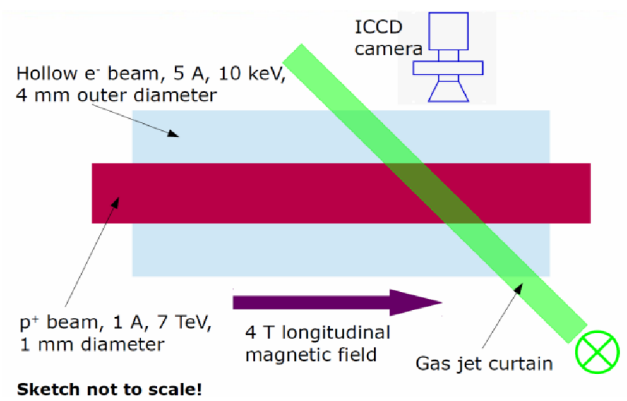


Figure 1: A schematic of the e-lens system planned at CERN for the collimation of the HL-LHC proton beam and the associated transverse beam diagnostics.

Fluorescence cross-sections and photon yield

For the gas jet curtain both neon and molecular nitrogen are under consideration. While N₂ is known for its high fluorescence efficiency, Ne has a better compatibility with high vacuum systems. Moreover the most prominent nitrogen lines originate from the N²⁺ ion, while neutral Ne has strong emission in the visible. This is relevant, since ion movement may get strongly affected by the electric and magnetic fields of the charged particle beams and the solenoid of the electron lens, in contrary to neutrals. Thus an extensive study has been conducted to predict the detectable photon rates to be expected for nitrogen and neon [2]. The results are summarized in Table 1.

First experimental results

Experiments with an electron beam and a nitrogen supersonic gas jet have been performed at the Cockcroft Institute. The gas jet setup generates gas sheets with a

width of several millimetres, sub-millimetre thickness and a particle density of about 10¹⁰ cm⁻³ [3]. An electron gun delivering up to 10 μA and a maximum energy of 5 keV is employed. BIF diagnostics is performed with an ICCD camera and a filter wheel with interference filters having a 10 nm bandwidth and central wavelengths at 337, 391, 431 and 471 nm.

Projectile	Jet	λ [nm]	σ [cm ²]	I [A]	N _γ [s ⁻¹]
electron	N ₂	337.1	1.5·10 ⁻²³	5	1.2
electron	N ₂ ⁺	391.4	9.1·10 ⁻¹⁹	5	7.5·10 ⁴
proton	N ₂ ⁺	391.4	3.7·10 ⁻²⁰	1	6.1·10 ²
electron	Ne	585.4	1.4·10 ⁻²⁰	5	2.9·10 ²
proton	Ne	585.4	4.7·10 ⁻²²	1	1.9

Table 1: Cross-sections σ and detectable photon rates for relevant nitrogen and neon lines. Protons are considered to have an energy of 7 TeV. The average proton beam current is 1 A. Electrons have an energy of 10 keV. The electron beam current is 5 A.

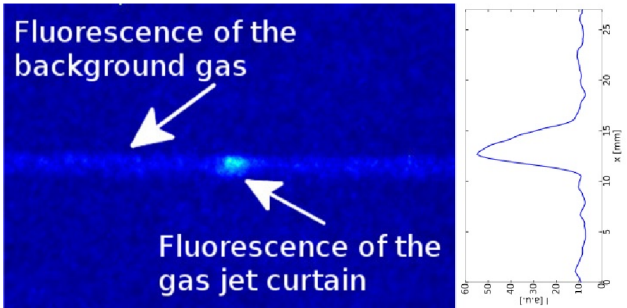


Figure 2: Profile of a 3.5 keV electron beam obtained due to the interaction with a supersonic N₂ gas jet curtain.

The profile of a 3.5 keV electron beam obtained due to the interaction with a nitrogen jet is shown in Fig. 2. The filter at 391 nm was used. Due to the very low electron beam current the integration time needed for good image quality has been 8000 s. Further investigations are planned for 2017.

References

[1] V. Shiltsev et al., Phys. Rev. STAB, **2**, 071001, 1999.
[2] S. Udrea et al., Proc. IBIC 2016.
[3] V. Tzoganis, and C.P. Welsch, Appl. Phys. Lett., **104**, 204104, 2014.



Ion source operation at GSI

R. Hollinger, K. Tinschert*, A. Adonin*, R. Berezov*, M. Brühl, B. Gutermuth, F. Heymach, S. Jung, R. Lang, J. Mäder, F. Maimone, K. Ochs, P. T. Patchakui, M. Raupach, P. Schäffer, S. Schäffer, C. Ullmann, C. Vierheller, A. Wesp, S. Zulauf*
GSI, Darmstadt, Germany

High Current Ion Sources

During the beamtime in 2016 a wide experimental program has been accomplished (realized) due to the parallel operation. High current ion sources from Terminal North (MUCIS and VARIS) and Penning ion sources from Terminal South were supplying the experiments with various types of ions. The following Table 1 gives an overview of the ion species, which were delivered for physics and accelerator development experiments. A representative value for delivered intensity to the linear accelerator UNILAC is the analysed beam current in front of the RFQ.

Table 1: Ion beam intensities generated with high current ion sources in 2016; filament driven volume type ion sources: MUCIS, vacuum arc ion sources: VARIS, Penning type ion sources PIG.

Ion species	Duration (days)	Ion source	Beam for experiment	Analyzed intensity (emA)
$^{15}\text{CH}_3^+$	18	MUCIS	UNI/SIS/ESR	2.4
$^{50}\text{Tl}^{2+}$	7	PIG	UNI	0.04
$^{124}\text{Xe}^{3+}$	19	MUCIS	SIS/ESR	2.6
$^{197}\text{Au}^{8+}$	23	PIG	UNI	0.07
$^{238}\text{U}^{4+}$	27	VARIS	UNI/SIS/ESR	16

The main requested ion species from the Penning Ion Source was gold $^{197}\text{Au}^{8+}$ for material research (UMAT) and for biophysics (UBIO) experiments. The PIG source was operated with high duty cycle (50 Hz / 3-4.5 ms) with the lifetime of approximately 24 hours during the beamtime.

One of the main highlights of the beamtime in 2016 was further performance optimization of VARIS ion source with multi aperture (7-holes, \varnothing 4 mm) triode extraction system for $^{238}\text{U}^{4+}$ beam. A new record for the beam brilliance in front of the HSI-RFQ has been achieved. An intensity of 13.5 mA (90% from full beam) was obtained inside the beam emittance of 178π mm·mrad horizontally and 175π mm·mrad vertically. Measured beam emittances for both planes are shown in Fig.1. Emittance measurements have been performed in UH1-section. In combination with tuning of the UNILAC high current injector (HSI) and the pulsed gas stripper [1] during the machine experiment campaign that results in a new record intensity of 11.5 mA for U^{29+} beam in the post-stripper section (US4-section) [2].

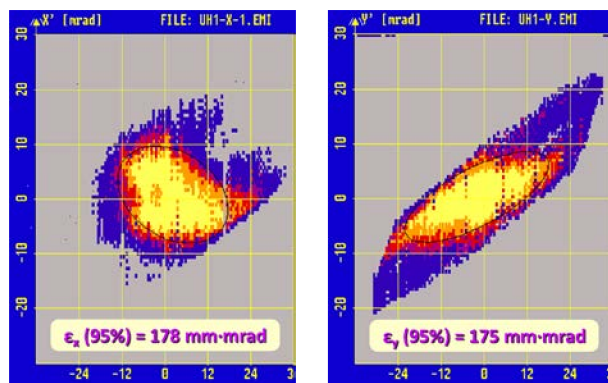


Figure 1: Measured emittances: horizontal (left) and vertical (right) of intense (15 mA) U^{4+} ion beam in front of the RFQ (UH1-section)

Another notable highlight is further development of molecular ion beams from Terminal North for production of intense proton and carbon beams behind the gas stripper [3]. A new separate gas-exhaust system for flammable gases has been developed and installed on terminal North. Due to this the production of CH_3^+ molecular ion beam from MUCIS ion source using methane gas has been established as standard operation. The optimization of the operation mode and the ion source parameters results in notably increased lifetime of MUCIS with methane.

In the frame of following elaboration of higher duty cycle (2.7 Hz) uranium operation for FAIR the investigation of possible ways of thermal load reduction of cathodes as well as the concept of using U-W composite materials in the cathodes is ongoing. The first set of test cathodes with U-W(5% Wt.) and U-W(12% Wt.) alloys will be manufactured by AREVA company [4] and delivered in the nearest future to GSI for performance tests with VARIS ion source on terminal North.

In the frame of the program of development of the new projectiles for FAIR experiments seven elements (including four new metals) have been successfully tested in various operation modes on terminal North in 2016 [5].

The further renewing and development of the Penning ion sources is in process. The five sputter PIG sources are completely renewed and successfully put into operation during this beam time. For the gas operation the renewing of PIG sources has been started. The first gas PIG source is ready and will be tested in the new constructed PIG test bench. Also the optimization and performance tests of compact PIG ion source are ongoing on the dedicated new test bench. The first results with argon beams are obtained.

* Corresponding authors

High Charge State Injector HLI

The CAPRICE ECR ion source (ECRIS) at the High Charge State Injector (HLI) experienced a major damage due to a lack of cooling during a test run at the end of 2015. In order to be prepared for the beam time of 2016 starting in April a big effort was made to reconstruct the ion source within the first quarter of the year. Due to the excessive temperature 3 of 6 coils of the ion source solenoids were destroyed, while the permanent magnet hexapole showed an intolerable decrease of magnetic remanence. Consequently these major components of the ion source had to be replaced. Fortunately most of the essential spare components were available for the required replacement. However, a complete disassembly of the ion source was inevitable and further components had to be refurbished or to be re-fabricated.

Table 1 shows the ion species delivered from the ECRIS during the regular beam time.

Table 1: Ion beam operation of the HLI-ECRIS in 2016

Ion species	Auxiliary gas	Duration (days)	Analysed intensity (eµA)
$^3\text{He}^{1+}$	He	12	500
$^{12}\text{C}^{2+}$	O ₂	12	160
$^{40}\text{Ar}^{9+}$	O ₂	19	100
$^{48}\text{Ca}^{10+}$	He	40	90-130

After the implementation of the CAPRICE-ECRIS at the HLI-LEBT a $^{40}\text{Ar}^{9+}$ ion beam was used for its re-commissioning at the HLI before the first beam time period. Subsequently this ion beam was used for tests and experiments scheduled at the cw-LINAC demonstrator [6] at the local experimental area of the HLI working at beam energies of 1.4 MeV/amu. A second period of experiments at the cw-LINAC demonstrator with $^{40}\text{Ar}^{9+}$ followed at the end of the beam time block.

Several short periods of biophysics experiments in 2016 were provided with ion beams of $^{12}\text{C}^{2+}$, and of $^3\text{He}^{1+}$, respectively.

A major part of the beam time was occupied by $^{48}\text{Ca}^{10+}$ beam which was delivered to various experiments on Super Heavy Element (SHE) research which were performed at TASCA and at SHIPTRAP, respectively. Most of the time a typical ion beam intensity of 90 eµA was provided while maximum intensities of 130 eµA could be achieved. The consumption of ^{48}Ca sample material was as low as 130 µg/h (including material recycling) in the first run and about 440 µg/h (without material recycling) during the high intensity period.

While for most of the elements produced as ion beams from the ECRIS a stable equilibrium can be found for a

favourable working point the situation can be more critical for the operation of ^{48}Ca . Occasionally the plasma is characterised by an unstable equilibrium but the response time for optimisation is very slow. For visual control purposes the plasma is continuously observed by means of a CCD camera equipped with a telephoto lens and looking through the straight beam line into the extraction aperture of the ion source which allows a close-up view of the plasma. Experiences obtained from ^{48}Ca beam times in the past years had shown that the colour of the plasma is mainly determined by the amount of Ca in the plasma. This is a critical parameter as it is correlated with the occurrence of instabilities. Moreover it could be verified that a change of colour already appears before an instability occurs. Therefore the monitoring of the colour could be helpful to anticipate instabilities early in order to intervene via re-optimisation. As the human eye is not capable to perceive small changes in colour the RGB values of the CCD-pixels are used. A small software tool has been set up which monitors the averaged RGB values of an area in the image which can be set by the software tool (yellow area in Figure 1a). A diagram visualises the trend of the RGB values over time (Figure 1b).

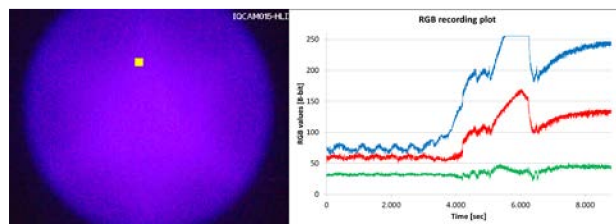


Figure 1: Camera image of the ^{48}Ca -plasma (a, left) and continuous RGB recording plot (b, right).

The application of this software tool during the last phase of the ^{48}Ca beam time showed promising results and turned out to be very helpful to simplify the optimisation of the ion beam.

References

- [1] W. Barth et al., U^{28+} -intensity record applying a H_2 -gas stripper cell, *Phys.Rev.STAB*, **18**, 040101 (2015).
- [2] W. Barth et al., High Brilliance Uranium Beams for FAIR, *Phys. Rev. Acc. Beams*, in print 2017.
- [3] A. Adonin et al., Production of high current proton beams using complex H-rich molecules at GSI, *Rev. of Sci. Inst.* **87**, 02B709 (2016).
- [4] AREVA GmbH, 91058 Erlangen.
- [5] A. Adonin, R. Hollinger, this report.
- [6] M. Miski-Oglu et al., GSI Scientific Report 2015, GSI Report GR-2016-1 (2016) 345.

UNILAC status report

*P. Gerhard*¹

¹GSI, Darmstadt, Germany

General remarks

As in 2015, the maximum ion energy of the UNILAC was restricted to 5.9 MeV/u due to the (planned) upgrade activities relating to the rf transmitters of the Alvarez tanks 3 and 4. The six operable single gap resonators were used for post acceleration several times, especially for synchrotron injection. Energy gains of up to $5.2(q/A)$ MeV/u were realized. For the first time the pulsed gas stripper was used over an extended period of four weeks in total, three of them during a regular ^{238}U beam time, successfully.

Operation

UNILAC operation started with machine checkout and commissioning on 4th April, regular operation began on 25th April and ended on 21st July. During commissioning ^{40}Ar beam was delivered for tests at the cw linac demonstrator. ^3He and ^{48}Ti were used for training and for commissioning of the ROSE setup in the transfer channel.

Regular beam time started with ^{197}Au (PIG), and with ^3He and ^{16}O (both ECRIS). This block was terminated early by a severe water incident in the HSI RFQ rf power amplifier, which was put out of operation for 10 days. Operation was resumed with ^{238}U (MeVVA) and ^{50}Ti (PIG) for UNILAC machine experiments. This was followed by the first block of ^{48}Ca (ECRIS) mainly for SHE experiments and $^{238}\text{U}^{63+}$ for the synchrotron and material sciences. After this, ^{197}Au , ^{12}C and again ^{197}Au were used alternately for three weeks by different users at the UNILAC, while $^{124}\text{Xe}^{43+}$ (MUCIS) was accelerated for the SIS. At the end of the Xe operation, another block of ^{48}Ca began. This was accompanied by ^{12}C made from CH_3^+ (CORDIS) cracked by the gas stripper. $^{12}\text{C}^{3+}$ and $^{12}\text{C}^{6+}$ were accelerated for the synchrotron. Later $^{12}\text{C}^{n+}$ together with $^1\text{H}^+$ also made from CH_3^+ were used for machine experiments at the UNILAC and SIS. The beam operation ended with ^{40}Ar for beam tests at the cw linac demonstrator and machine experiments with ^{238}U and ^{50}Ti .

Aged capacitors in magnet power converters caused a number of breakdowns, including one severe incident where all IGBT modules of a kicker magnet PC were damaged. This almost terminated the beam time. A failure of a power supply of the UNILAC emergency stop caused a shutdown of the complete accelerator, and one day was lost.

Despite the several serious failures, the beam operation of the UNILAC was quite successful, thanks to the great effort of all colleagues involved.

Shutdown Activities

The renewal of the power converter for the Alvarez tank 3 rf transmitter was continued throughout the year. The replacement of the Alvarez tank drift tubes no. 30 of tank 1 and no. 15 of tank 3 started in November 2015 and was finished end of February 2016. In January a water leakage occurred at a baffle in the HLI beam line. It was not immediately noticed, because the vacuum system was switched off for maintenance reasons. A gate valve was erroneously opened, probably due to a defective vacuum controller. This caused flooding of a larger part of the beam line up to the gas stripper section, including two rf cavities and several vacuum pumps. The whole beam line was dismounted, disassembled, inspected and cleaned. One turbo pump was damaged. In spring, the field stabilization of all dipole magnets at the TK charge state separator was improved by new Hall probes.

After the beam time, the exchange of the last inner tank triplet of the first IH tank at the high current injector (HSI) began (ground fault). The adaptor plate was damaged during copper plating, a new plate will be delivered in May 2017. Several breakdowns of magnet power converters happened during operation (s. a.). A major replacement and maintenance programme will be executed until 2018.

The 108 MHz buncher TK4BB11 was out of operation, because its rf power line had been flooded partly by water from a defective coupling loop before the beam time. This was no constraint for operation, the repair is ongoing.

Machine Experiments

Machine experiments with the pulsed gas stripper were conducted in May and July, using ^{238}U , ^{50}Ti , and ^1H and $^{12}\text{C}^{n+}$ from CH_3^+ [1, 2]. The amplitude calibration and beam loading effects of the single gap resonators were investigated with ^3He and ^{124}Xe respectively. Several measurements with ROSE were conducted in the transfer channel with ^3He and ^{238}U . High current measurements regarding the FAIR beam requirements were performed with ^{238}U and ^1H all along the UNILAC [2]. At the entrance to the transfer channel, 5.4 mA of $^{238}\text{U}^{28+}$ and 3.6 mA of $^1\text{H}^+$ were achieved.

References

- [1] P. Scharrer et al. (this report)
- [2] Report on UNILAC Machine Experiments, LINAC dept., www.gsi.de

Status of the pulsed gas stripper for the UNILAC

P. Scharrer^{1,2,3}, W. Barth^{1,2}, M. Bevcic², Ch. E. Düllmann^{1,2,3}, P. Gerhard², L. Groening², K. P. Horn², E. Jäger², J. Khuyagbaatar^{1,2}, J. Krier², H. Vormann², and A. Yakushev²

¹HIM Helmholtz-Institut Mainz, Mainz, Germany; ²GSI Gesellschaft für Schwerionenforschung GmbH, Darmstadt, Germany; ³Johannes-Gutenberg Universität, Mainz, Germany

The GSI UNILAC will be used as part of the injector chain for FAIR [1]. In order to meet the high demands in terms of delivered beam current and quality an extensive upgrade program of the UNILAC is ongoing [2]. In this process a new setup for the gas stripper at 1.4 MeV/u was developed [3] and has been first employed in 2014. A pulsed gas injection is used instead of the continuous gas-jet of the previously existing stripper setup. With this setup, using H₂-gas, and together with additional improvements, significantly increased uranium beam intensities were achieved behind the gas stripper [4].

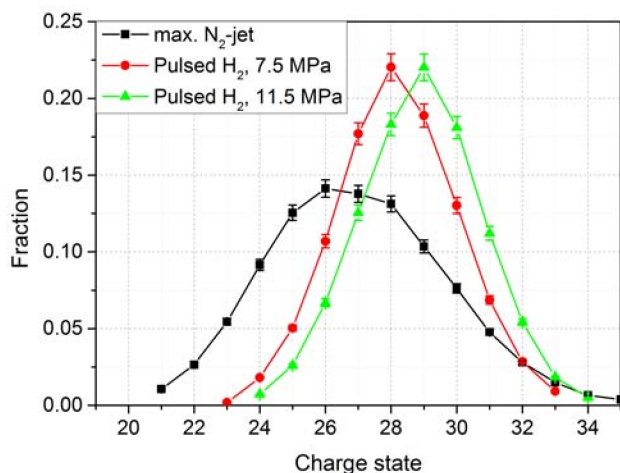


Figure 1: Comparison of the charge state distributions of ²³⁸U ions after passing through the charge stripper applying different gas targets and back-pressures on the gas inlet.

Recent measurements

In 2016, additional measurement series were conducted over five days of machine beam time. The main topic was to obtain complete data sets for stripping of uranium and titanium beams, complementing measurements conducted in 2015, and additional measurements of the beam properties behind the gas stripper. For high-current measurements the VARIS-type ion source [5] was used and optimized for high-current operation. With the pulsed gas stripper, using H₂-gas, the target thickness can be adjusted to shift the maximum of the charge state distribution of uranium either to charge state 28 or 29 (see Fig. 1).

Measurements of charge state distributions of uranium and titanium beams after passing through different gases at 0.12 MeV/u and 0.74 MeV/u beam energy were conducted.

To enable measurements at lower beam energies, the DTL tanks of the HSI were turned off separately. The corresponding results for 0.74 MeV/u are presented in [6]. At 0.12 MeV/u beam energy, the major part of the charge state distribution could not be measured due to limitations of the magnetic field of the dipole magnet in the charge separation system.

Additionally, the optimal target thickness for operation with the titanium beam was determined to reach maximum yield into a desired charge state. Due to limitations of the differential pumping system, this target thickness is currently not viable in long-pulse operation mode (5 ms pulse length, 50 Hz repetition rate). Alternatively, N₂-gas can be used with the pulsed gas stripper to match the performance of the previously existing N₂-jet stripper setup.

Long-term test

The pulsed gas stripper setup has been used continuously for three weeks during the SIS18 beamtime as a long-term test. During this time, the UNILAC delivered high-intensity U²⁸⁺-ion beams. A pulsed H₂-gas target with a thickness of about 9 μg/cm² was used.

After about two weeks, an increased gas pressure in the adjacent accelerator structures was noticed, which caused the closure of the adjacent gate valves. This was found to be due to a leaky gas valve, which had been in use as the main gas inlet for about 15 days in the course of several beam times and offline measurements in 2015-2016. After switching to the second gas valve, which had significantly less duty time in the past, the beam time continued without any further incidents due to the gas stripper. Additional systematic long-term measurements with the pulsed gas valves are in preparation at a dedicated test stand to identify the cause of this outage.

References

- [1] FAIR Baseline Technical Report, Vol. 2, GSI Darmstadt, Germany p. 335 (2006).
- [2] L. Groening et al., in proceedings of IPAC2016, Busan, Korea (JACoW) MOPOY017 (2016).
- [3] P. Scharrer et al., in proceedings of IPAC2016, Busan, Korea (JACoW) TUPMR058 (2016).
- [4] W. Barth et al., Phys. Rev. Accel. Beams 18 040101 (2015).
- [5] R. Hollinger et al., Nucl. Instrum. Meth. B 239 p. 227 (2005).
- [6] P. Scharrer et al., Phys. Rev. Accel. Beams 20, 043503 (2017).

Pressure profile simulations for UNILAC gas stripper

P.M. Suherman, P. Gerhard, M. Maier, M.C. Bellachioma, J. Cavaco, M. Kaiser
GSI, Darmstadt, Germany.

Introduction

A new gas stripper setup based on a pulsed gas injection is being developed at GSI UNILAC. This work is part of an upgrade of the existing gas stripper in preparation for the FAIR project [1]. The inlet pressure of the pulsed gas will be in the order of 100 bar. The gas will flow through the nozzle and disperse through the T-pipe construction in the gas stripper chamber (Figure 1). It is expected that the gas flow will then be directed to the pipes/apertures connecting the gas stripper chamber and the adjacent differential pumping chambers. The purpose of the new gas stripper is to maximise the gas density inside the T-pipe, in order to increase the stripping efficiency. During this process, the gas flow from the stripper chamber to the adjacent chambers connected to the accelerator must be kept as low as possible. A pressure profile simulation is therefore conducted to investigate if a new design of the gas stripper may be used to improve the stripping performance, as well as maintaining a sufficient low pressure for the neighbouring accelerator sections for high duty factors.

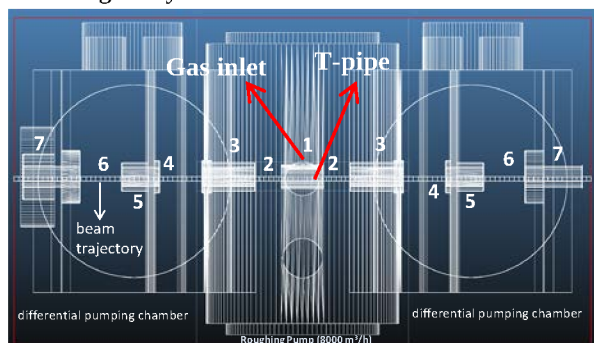


Figure 1: Cross-section of gas stripper chambers.

Pressure Profile Simulations

The gas stripper setup consists of a gas stripper chamber and two differential pumping chambers that are connected to the accelerator sections. All chambers have dimensions of approximately 20 cm diameter and 30 cm long. The chambers are all linked via ~ 2 cm diameter pipes/apertures, which are positioned in the middle of the chambers at the beam trajectory (see Figure 1).

The gas stripper chamber itself consists of a T-pipe construction with a fast switchable nozzle as high pressure gas inlet. The T-pipe is mounted directly in-line with the pipes/apertures connected to the adjacent chambers. A roughing pump with a pumping speed of 8000 m^3/h is mounted directly underneath the T-pipe.

The differential pumping chambers are equipped with 4 turbo pumps (1200 l/s – N_2 equivalent). These high speed pumps are required in order to achieve a sufficiently low pressure ($<10^{-6}$ mbar) in the accelerator sections.

The pressure profile was calculated using a Monte Carlo based simulation for vacuum conditions (Molflow software) [2]. A N_2 gas pulse of 1 Hz repetition rate and 100 μs pulse length and two different gas flow rates were used in the simulation: 1 mbar·l/s and 10^4 mbar·l/s.

Figure 2 shows the pressure profiles along the beam trajectory. The preliminary simulation results show that there should be a sufficient gas density inside the T-pipe, while maintaining low enough pressure in the differential pumping chambers. For a low gas flow rate (1 mbar·l/s), the pressure inside the T-piece pipe is approximately 5×10^{-6} mbar. The pressure will increase proportionately with the gas flow rate. The anticipated gas flow rate to be used is in the order of 10^4 mbar·l/s. Therefore, the pressure inside the T-piece will be approximately 5×10^{-2} mbar.

The concern with using higher gas flow rates is that the pressure in the differential pumping chambers is increasing above the limit for the accelerator sections. At a gas flow rate of 10^4 mbar·l/s, the pressure in the differential pumping chambers is in the order of 10^{-3} mbar (inside the pipe/aperture) - 10^{-4} mbar (outside the pipe/aperture). This pressure is considerably too high, since these chambers are directly connected to the accelerator sections.

A possible simple solution to obtain a low pressure in the differential pumping chambers while maintaining the optimum gas density in the gas stripper is the use of higher pumping speed for the turbo pumps. This will be investigated in the future simulation work.

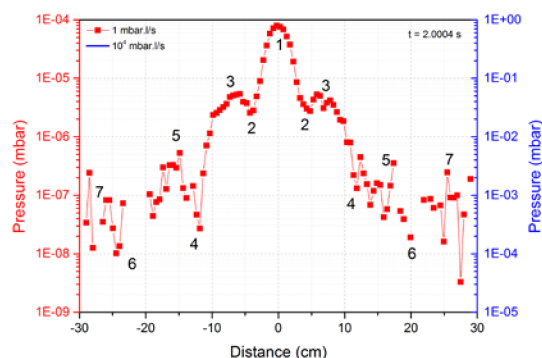


Figure 2: Pressure profile along the cross-section of the chamber for a pulsed N_2 gas

The drawback of using Molflow software for this purpose is the inaccuracy that may be observed in the area of the T-piece by the gas injection, due to a viscous flow. A future work may use ANSYS software to compare the pressure profiles for this setup.

References

- [1] P. Scharrer, et. al. J. Radional. Nucl. Chem., 2015.
- [2] <http://molflow.web.cern.ch/content/about-molflow>.

Status of the 108 MHz RF system modernisation at the UNILAC

B. Schlitt, J. Catta, T. Eiben, G. Eichler, S. Hermann, M. Hörr, F. Lorenz, M. Müh, S. Petit, M. Pilz, E. Plechov, J. Salvatore, R. Scholz, G. Schreiber, W. Vinzenz, A. Windolf, and J. Zappai

GSI, Darmstadt, Germany

Modernisation of existing RF systems

Various tests of the modernised RF system at the Alvarez tank 3 were successfully performed during 2016. It comprises the rebuilt high power RF amplifier stage (HPA), a new separate control rack (including a newly developed measurement and fast interlock unit and a commercial control grid power supply), and the updated 1 MVA, 24 kV anode power supply equipped with a new PLC control [1, 2].

A specifically developed manual control unit is used for test operation of the HPA. For routine operation, another PLC system based on Siemens S7-1500 is being built and programmed (Fig. 1) [3]. The system handles monitoring and interlocks of all HPA cooling circuits and power supplies, turn-on/off sequences of the supply voltages, system access interlocks, control of the motorized tuning circuits, basic switch-on/off commands of the driver amplifier and of the LLRF output signal, etc. The central part of the PLC is installed in the separate control rack, whereas a subunit is directly installed in the HPA stage comprising the I/O modules for all signals provided there. The PLC system as well as the manual control unit is designed for both amplifiers – the existing HPA as well as the new Thales amplifier (see below). First prototype tests of the new PLC system were performed at a test set-up [3]. Tests of the final PLC system installed in the Alvarez 3 RF system are scheduled for summer 2017.

The fully modernised Alvarez 3 RF system as well as the upgraded 1 MVA anode power supplies at Alvarez 1–3 will be used for routine operation during the beam time 2018. The remaining HPA stages will be upgraded in the same way.

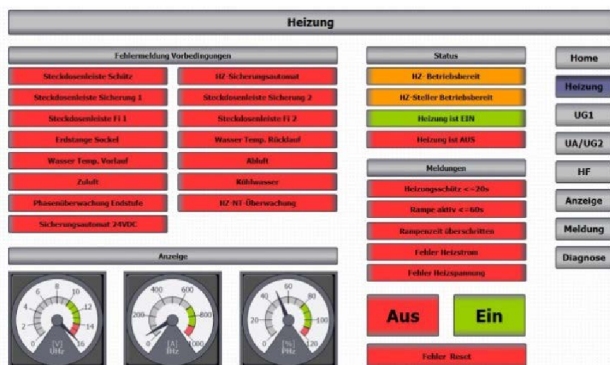


Figure 1: PLC system graphical user interface for filament operation at the Alvarez high power RF amplifiers.

New 1.8 MW cavity amplifier prototype

The new 1.8 MW cavity amplifier prototype [1] was commissioned successfully at Thales Electron Devices [2, 4]. The manual control unit developed by GSI was

used for the tests to control interlocks and the motorised tuners. Parasitic oscillations which occurred around 900 MHz could be damped successfully by placing EC-COSORB MF-124 bars at the bottom of the output circuit of the cavity [4]. Further tests and measures were taken to ensure good suppression of parasitic oscillations during pulsed operation [2, 4]. Finally, the factory acceptance tests (FAT) were successfully finished in July 2016 including a 3×8 hour test run at 1.8 MW peak RF output power on dummy load without any trip.

After delivery to GSI, the new amplifier was integrated into the existing equipment at the UNILAC RF gallery (anode power supply, driver amplifier, air and water cooling systems, installation of RF transmission lines, etc.) and a control rack similar to that built for the A3 amplifier was installed (Fig. 2). An existing huge coaxial transmission line switch in the output RF line is used to switch between a water dummy load and the Alvarez tank 4 at the UNILAC. Site acceptance tests (SAT) at GSI are scheduled for July – August 2017. Routine operation of the new amplifier on Alvarez tank 4 is planned during regular beam time from 2018 on.



Figure 2: New 1.8 MW high power cavity amplifier prototype installed at the UNILAC RF gallery plus control rack equipped with grid power supplies, new measurement & fast interlock unit, and further control elements.

References

- [1] B. Schlitt et al., GSI Scientific Report 2015, p. 310.
- [2] B. Schlitt et al., LINAC2016, THPLR025.
- [3] S. Petit, Bachelor Thesis, Darmstadt University of Applied Sciences (Hochschule Darmstadt), Darmstadt, Germany, 2016.
- [4] Thales Electron Devices, Thonon-les-Bains, France.

Design study for a first of series Alvarez-cavity

M. Heilmann^{*1}, *X. Du*¹, *P. Gerhard*¹, *L. Groening*¹, *M. Kaiser*¹, *S. Mickat*¹, *A. Rubin*¹, and *A. Seibel*²

¹GSI Helmholtzzentrum, 64291 Darmstadt, Germany; ²IAP, Frankfurt University, 60438 Frankfurt am Main, Germany

The design study describes the first of series Alvarez tank of the new poststripper section as injector for FAIR. The existing Alvarez linac had an operation period of over 40 years and the repair efforts increase particularly with regard to the drift tubes and the included magnets. The FAIR experiments have new requirements to the linac and a high availability is important for the new main operational injector [1]. The UNILAC at GSI comprises a low energy section with RFQ and IH-DTL with an energy of 1.4 MeV/u and after the stripper section the Alvarez-DTL accelerates the design beam of U^{28+} up to 11.4 MeV/u and delivers the beam to the SIS18. In the first step a first of series Alvarez tank (Table 1) with 11 drift tubes (quadrupole singlets are included) and a total tank length of 1.9 m will be manufactured (Fig. 1). This cavity will implement the new drift tube shape profile to increase the shunt impedance and a new beam dynamics concept [2, 3]. Furthermore it is possible to investigate an optimized stem position to increase the RF-field stability [4]. After low level measurements the prototype will be conditioned and operated with high power.

pling and a maintenance hole are installed in the bottom. In the center position on the tank side are installed two vacuum pumps. The Alvarez tanks will all have these parts at the bottom. The frequency range is increased with eight tuners in total (two dynamical tuners).

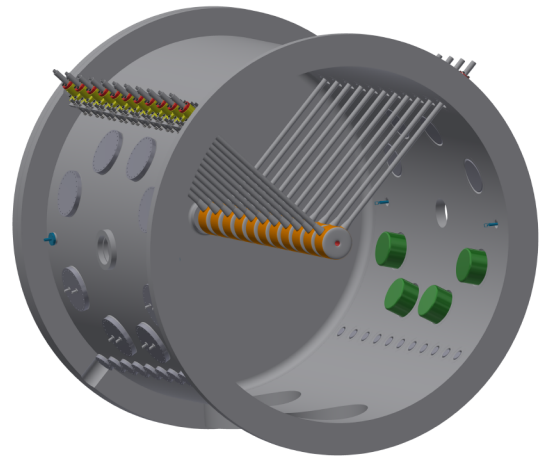


Figure 1: CAD-model of the first of series Alvarez tank with a length of 1.9 m and 11 drift tubes.

Table 1: Parameters of the first of series Alvarez tank

Parameter	Unit	Value
Frequency	MHz	108.408
A/q		≤ 8.5
max. Current	mA	16.5
Synchronous Phase	deg.	-30
RF-pulse length	ms	2
Beam repetition rate	Hz	10
Input energy	MeV/u	1.4
Output energy	MeV/u	1.7
Gaps	#	12
Gap length	mm	40.9-44.7
Drift tubes	#	11
Drift tube length	mm	111.3-122.2
Drift tubes diameter	mm	180.0
Aperture	mm	30.0
Tank diameter	mm	1948.9
Tank length	mm	1917.2
Q - Factor		82000

Mechanical Integration

The drift tubes are installed from the top of the tank (Fig. 2), but other combinations are possible [4]. RF cou-

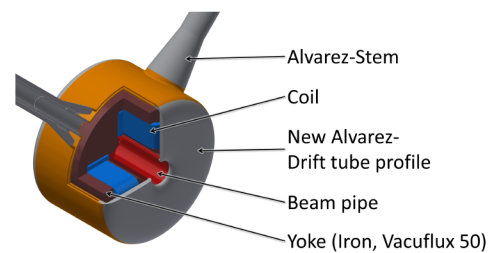


Figure 2: Alvarez-drift tube with the new shape profile. In the drift tube casing a water cooling system is implemented. The power and water supply for the magnet is in one Alvarez-stem only. Both stems and the casing of the drift tube are cooled.

References

- [1] L. Groening et al., Upgrade of the Universal Linear Accelerator UNILAC for FAIR, MOPOY017, Proceedings of IPAC'16, Busan, Korea, p. 880 (2016).
- [2] X. Du et al. (this report)
- [3] A. Rubin et al. (this report)
- [4] X. Du et al., DOI: 10.1103/PhysRevAccelBeams.20.032001

*m.heilmann@gsi.de

Status of the beam dynamics design of the new post-stripper DTL

A. Rubin¹, X. Du¹, L. Groening¹, and S. Mickat¹

¹GSI, Darmstadt, Germany

Introduction

The GSI UNILAC has served as injector for all ion species since 40 years. Its 108 MHz Alvarez DTL providing acceleration from 1.4 MeV/u to 11.4 MeV/u has suffered from material fatigue and has to be replaced by a new section [1]. The design of the new post-stripper DTL is developed in GSI [2]. Five Alvarez tanks with four intertank sections provide 100% transmission and low emittance growth. The intertank sections allow for a matched solution and provide place for diagnostics [3].

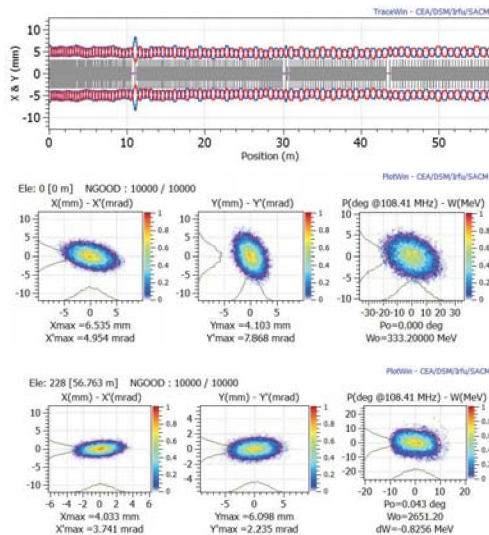


Figure 1: FAIR case: envelopes along the new Alvarez-DTL, input and output distributions.

Beam dynamics simulations for the new Alvarez DTL

The beam dynamics simulations for the new model were done for $^{238}\text{U}^{28+}$ using the TraceWin code [4]. The behaviour of the beam in the proposed structure was investigated for different zero current phase advances, as without current, as for the current of 16.5 mA. Input emittances were chosen as $E_x=E_y=0.175$ mm·mrad and $E_z=70$ deg·keV/u. Simulations along the complete Alvarez DTL (Fig. 1) were done for the zero current phase advance of 65° for each tank. The intertank section for the presented design consists of quadrupoles, one buncher, and spaces between them. These drifts can be filled with other elements (trafo, steerer, grid, probe etc.) The 1st and the 3rd quadrupoles are placed partially in the tank cover, the length of the intertank section is about 1m. The total emittance growth for the whole Alvarez is about 7%. The new DTL serves also for the non-FAIR scenarios. Results of beam dynamics simulations for six different scenarios including the FAIR nominal case and low energy operation are presented in Tab.1.

References

- [1] L. Groening, et al. "Upgrade of the Universal Linear Accelerator UNILAC for FAIR", IPAC 2016, Busan, Korea, Mar. 2016, paper MOPOY017, pp. 880-882
- [2] X. Du, et al. "Alvarez DTL Cavity Design for the UNILAC Upgrade", IPAC 2015, USA
- [3] A. Rubin, et al. "Status of beam dynamics design of the new post-stripper DTL", annual report 2015, GSI
- [4] TraceWin <http://irfu.cea.fr/Sacm/logiciels/index3.php>

Table 1: Six investigated cases for the new Alvarez DTL:

	FAIR case	Zero current	Low Energy	Larger Long.	Smaller Long.	Transvers. Flat
I, mA	16.5	0	0	16.5	16.5	16.5
E_x (rms), mm mrad	0.175	0.175	0.175	0.175	0.175	0.0875
E_y (rms), mm mrad	0.175	0.175	0.175	0.175	0.175	0.35
E_z (rms), MeV/u deg	0.07	0.07	0.07	0.14	0.035	0.07
Energy (out), MeV/u	11.4	11.4	3.3	11.4	11.4	11.4
Transmission	100%	100%	100%	100%	100%	100%
δE_x (tot, 95%)	7%	0%	0%	7%	8%	16%
δE_y (tot, 95%)	7%	0%	0%	10%	7%	3%
δE_z (tot, 95%)	10%	0.7%	1.7%	5%	11%	4%
Bunch Length (95%)	± 16 deg	± 11 deg	± 33 deg	± 21 deg	± 14 deg	± 17 deg

Benchmarking of four post-stripper DTL options

S. Mickat, L. Groening, A. Rubin

GSI, Darmstadt, Germany

After more than 40 years of reliable operation the existing post-stripper DTL commences causing an increasing amount of down time of the GSI facility as well as of the amount of resources for repair and maintenance. In 2013 an evaluation of options for refurbishment drew the conclusion that the amount of related resources does not justify this activity. Moreover, in 2013 a dedicated review by external experts stated that the present layout of the post-stripper will not allow for reaching FAIR's requirement to its injector linac. The results from 2013 were confirmed by a 2nd review in 2016, where the listed four post-stripper DTL options were reviewed:

- new Alvarez DTL
- KONUS IH DTL
- synchronous IH DTL
- refurbishment of existing Alvarez DTL

The two first listed DTL concepts passed the review as being feasible from first principles. The required resources for installation of a new post-stripper DTL are similar for the two DTL concepts. The KONUS IH has lower cost but its final beam quality does not comply with the FAIR requirements. Therefore the Alvarez option has been favoured in-house.

In preparation of the review, which took place in October 2016, common rules w.r.t. obtaining information as well as a schedule and deliverables towards a reliable benchmarking were defined three months before. In two dedicated meetings in August chaired by the Accelerator Operation division head, these rules, the data exchange format, and six beam dynamic benchmark scenarios including input particle distributions were communicated to those collaborations that proposed an option.

The most important scenario is conceived to check the option's ability to serve as a dedicated FAIR injector. Two scenarios assume different initial longitudinal beam parameters, while two additional scenarios probe the beam requirements of today's UNILAC experiments. The 6th scenario is on the compliance with future upgrade measures based on flat beam injection into the SIS18. In parallel to the beam dynamics investigations a systematic cost estimate by GSI experts for the four options has been conducted.

The table below presents an extraction of the obtained data and information, which was sent to the review committee prior to the review itself. The complete table lists 43 items and the report on the cost estimate comprises 42 pages. In February 2017 the GSI/FAIR directorate decided that the Alvarez option will be followed exclusively.

Table 1: Extract of the table which summarizes the benchmarking results.

Criteria	New Alvarez	IH (KONUS)	IH (synchronous)	Alvarez (refurbished)
FAIR injection				
Transmission [%]	100%	100%	100%	-
Final emittances (95% tot., norm.)	1.058 mm mrad 1.061 mm mrad 104.19 MeV deg	1.62 mm mrad 1.64 mm mrad 107 MeV deg	1.262 mm mrad 1.228 mm mrad 111.67 MeV deg	-
Final bunch length (95% tot.)	± 16 deg	± 16 deg	± 26 deg	-
Flat beam injection				
Transmission [%]	100%	99.4%	-	-
Final emittances (95% tot., norm.)	0.575 mm mrad 2.033 mm mrad 97.09 MeV deg	1.19 mm mrad 2.36 mm mrad 109.82 MeV deg	-	-
Final bunch length (95% tot.)	± 17 deg	± 14 deg	-	-
General parameters				
DTL length [m]	57 (+4m Transferline)	23 (+38 m Transferline)	35 (+26m Transferline)	
Eff. gradient [MV/m]	1.59	3.76	2.77	
# cavities	5x Alvarez 4x Buncher	5x IH DTL	20x IH DTL	5
(Transferline)	(-)	(3x Buncher)	(1x IH-DTL)	
Costs				
[M€]	28.4	18.3	40.3	> 25.1

Status of the IH-DTL poststripper linac proposal*

H. Hähnel[†], U. Ratzinger, and R. Tiede

Institut für Angewandte Physik, Goethe Universität Frankfurt

Motivated by the necessary replacement of the GSI UNILAC poststripper linac, a compact and efficient linac design based on IH-type cavities has been developed [1, 2]. Using KONUS beam dynamics, it was possible to design a linac consisting of only five cavities that can be operated by the existing UNILAC RF amplifier structure. The transversal focusing scheme is based on magnetic quadrupole triplet lenses.

The optimized design provides full transmission and low emittance growth for the design current of 15 emA U^{28+} , accelerating the beam from 1.4 MeV/u to 11.4 MeV/u. Extensive error studies were performed to define tolerances and verify the stability of the design with respect to misalignment and injection parameters. With a total length of just 22.8 meters, the design provides a compact and cost effective alternative to a new Alvarez linac.

Error Studies

Extensive error studies were performed on the IH-DTL poststripper linac design using TraceWin. The total number of simulated particles for each simulation run is 10^7 to 10^8 . These values were chosen to achieve reproducible results. A detailed description of the error studies can be found in [1], including:

- Sensitivity studies of the individual component errors (magnetic lenses, cavities, RF, beam)
- Error studies of different combined error sets
- Finding the best steering strategy
- Influence of corrective steering on error tolerance

Based on the sensitivity studies, simulations were performed with combined error sets (see Tab. 1). Case A resembles the error limits beyond which significant losses and/or emittance growth were observed in the sensitivity studies. In Case B, only the magnetic triplet errors are reduced to $\Delta xy = 100 \mu\text{m}$ and $\Delta\phi_{x,y,z} = 1 \text{ mrad}$ to account for strong coupling of singlet and triplet errors. For Case C, all errors were reduced to optimistic achievable values. The resulting additional emittance growth and average transmissions for these three error sets are summarized in Table 2. As expected, the “Case A” error set shows significant average losses. Due to strong coupling between quadrupole singlet and triplet errors, the average transmission of “Case B” is significantly improved. Even without

Table 1: Lens parameters for combined error runs of the poststripper IH-DTL (cavity/RF errors not shown [1]).

Error Type	Case A	Case B	Case C
Quadrupole Lenses			
Singlet Δxy	80 μm	80 μm	50 μm
Singlet $\Delta\phi_{x,y,z}$	1 mrad	1 mrad	1 mrad
$\Delta B'/B'_0$	0.7 %	0.7 %	0.1 %
Triplet Δxy	360 μm	100 μm	100 μm
Triplet $\Delta\phi_{x,y,z}$	1.6 mrad	1 mrad	1 mrad

any corrective steering in the linac, an average transmission of 99.76 % is achieved for the Case C.

After investigation of different steering strategies, it was found that a total of four steerers, set up as two steerer pairs, is sufficient for the proposed linac. With this steering strategy, the average losses can be significantly lowered from 7.21 % to 0.03 % for Case A (see Tab. 2). In combination with strict error tolerances, as in Case C, the losses can be reduced even further to $6 \cdot 10^{-8}$.

Table 2: Resulting additional emittance growth and losses of combined error simulations with and without steerers.

	$\Delta\epsilon_x$ [%]	$\Delta\epsilon_y$ [%]	Losses [%]
Case A	1.0 %	0.2 %	7.2 %
Case B	2.1 %	2.1 %	1.5 %
Case C	0.6 %	1.3 %	0.2 %
with steerers:			
Case A	1.4 %	2.5 %	0.03 %
Case C	0.7 %	0.8 %	$6 \cdot 10^{-8}$

References

- [1] H. Hähnel, “Development of an IH-Type Linac for the Acceleration of High Current Heavy Ion Beams”, Ph.D. thesis, Phys. Dept., Goethe University, Frankfurt, Germany, 2017.
- [2] H. Hähnel, U. Ratzinger, R. Tiede, “Status of the IH-DTL Poststripper Linac Proposal”, GSI Scientific Report 2015, p. 300.

* Work supported by BMBF05P15FRBA

[†] haehnel@iap.uni-frankfurt.de

Simulation of UNILAC BPMs with CST

R. Singh¹, P. Forck¹, W. Kaufmann¹, T. Sieber¹, T. Reichart¹, and J. He²

¹GSI, Darmstadt, Germany; ²IHEP, Beijing, China

Several BPMs are installed in GSI UNILAC to monitor beam positions with a desired resolution of at least 1 mm at a rate of 1 MHz. Initial stages of UNILAC e.g. RFQ and IH structures operate at 36 MHz while the later part i.e. Alvarez part operates at 108 MHz. The processing electronics utilize 72 MHz for one BPM placed at the exit of RFQ and 216 MHz for rest of the BPMs. These BPMs were simulated to calculate the position sensitivity at the processed frequency.

Simulations and results

Figure 1 shows the CST model for top part of the BPM plates. The pick-ups have a rather complex design for reasons such as protection from beam hits, good position sensitivity as well as mechanical stability.

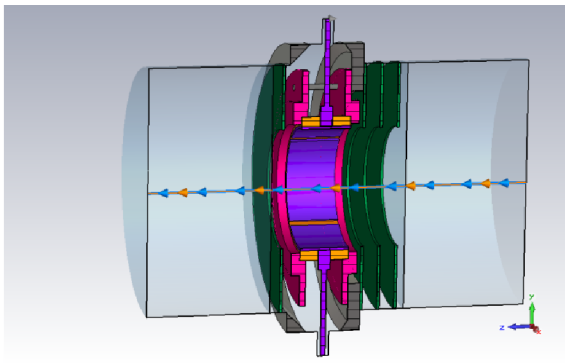


Figure 1: Model of UNILAC BPM as simulated in CST.

Scattering parameters of the structure were measured by a network analyzer as shown in Fig. 2 where S21 represents the coupling to the opposite plate and S31 is the coupling into the another plane, and S11 is the reflection. The corresponding S-parameters derived from the simulation are shown in Fig. 3 and closely matched the measured parameters which confirmed the pick-up model and gave insights into the crucial components of the design. Figure 4 shows the position sensitivity of the pick-up calculated for a relativistic beam; the percentage change in difference signal of the opposite plates as a function of beam position. The coupling between opposite plates (as characterized by S21) increases with frequency which explains the observation that the position sensitivity decreases with increasing frequency. The coupling from one plane to another (S31) has a peak at around 200 MHz which reduces the position sensitivity and modifies the shape of sensitivity curve to bring a non-trivial position dependence. The outlook is to confirm the results with the more relevant case of non-relativistic beams in different sections of UNILAC.

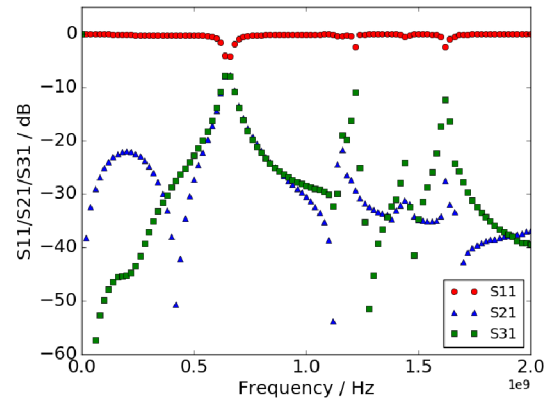


Figure 2: Measured S parameters.

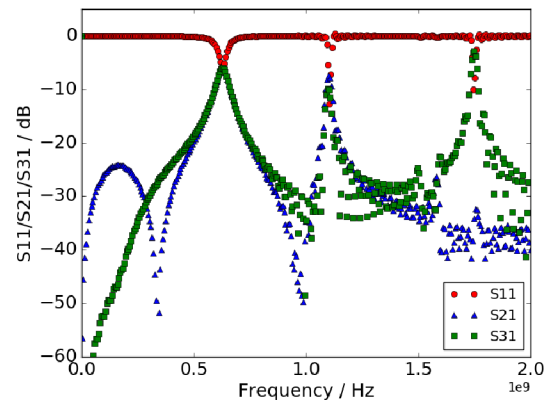


Figure 3: Simulated S parameters.

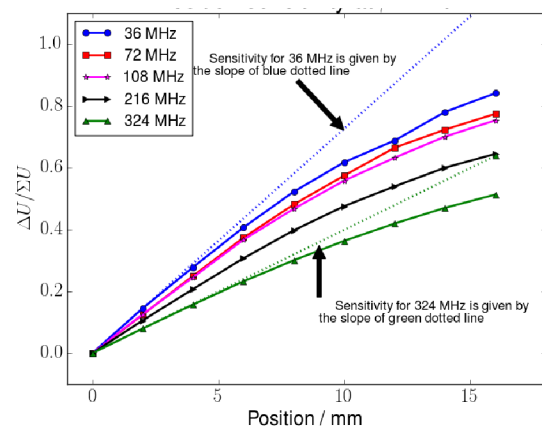


Figure 4: The slope of the curves correspond to position sensitivity at the respective frequency.

Structural mechanical simulations for a new 108 MHz CW RFQ for the HLI*

D. Koser^{†1}, P. Gerhard², L. Groening², O. Kester³, and H. Podlech¹

¹IAP, University of Frankfurt, Germany; ²GSI, Darmstadt, Germany; ³TRIUMF, Vancouver, BC, Canada

The currently operated 108 MHz 4-rod RFQ at the HLI was commissioned in 2010 [3]. Unfortunately the structure suffers from strong modulated RF power reflections with a frequency of approximately 500 Hz that severely limit the achievable pulse length and amplitude [2]. Measurements of the velocity profile of the electrodes using a laser vibrometer identified mechanical vibrations as source of the RF modulations and additionally revealed other vibrational modes around 350 Hz that however do not affect the RF behavior [1]. In structural mechanical simulations using ANSYS Workbench the measured frequency spectra could be replicated accurately. Derived concepts for the mitigation of the RF affecting mechanical eigenmodes were implemented in the design of a prototype for a completely revised 4-rod HLI-RFQ.

Mechanical Eigenmodes

It could be shown that the RF affecting vibrations at 500 Hz correspond to radial oscillations of the electrodes that are triggered by the radially acting electric forces of the quadrupole field. Tangential oscillations with eigenmode frequencies of roughly 350 Hz are caused by asymmetries (e.g. dipole component) and are therefore comparatively small, having an negligible influence on the RF properties.

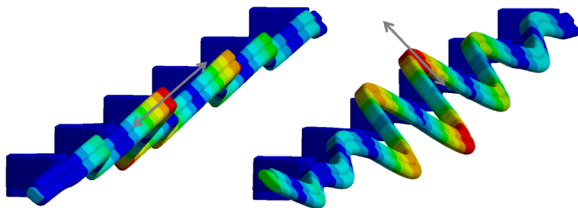


Figure 1: Mechanical eigenmodes of the electrodes

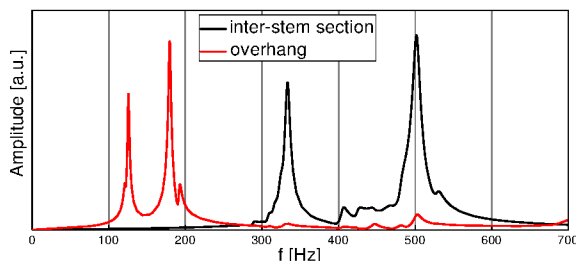


Figure 2: Simulated mechanical resonance spectrum of the inter-stem electrode sections (black) and the overhang (red)

* work supported by BMBF Contr. No. 05P15RFRBA

[†] koser@iap.uni-frankfurt.de

Prototype Development

Starting from the basic FRANZ/MYRRHA-RFQ concept the electrode profile, trapezoidal electrode mountings, stem geometry and stem distance were optimized in view of mechanical rigidity, shunt impedance and electric dipole. The resonance frequencies of the mechanical eigenmodes could be increased by a factor of roughly 4 compared to the existing HLI-RFQ while mostly preserving the value of the shunt impedance of about 100 k Ω ·m. The electric dipole is compensated entirely.

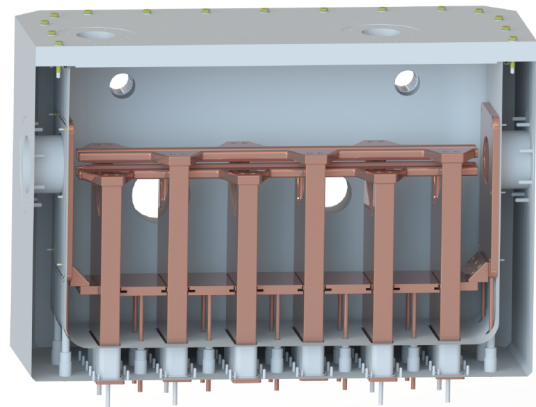


Figure 3: Final 6-stem prototype design

From a previously intended 4-stem design the prototype configuration was upgraded to 6 stems in order to reproduce a mechanical resonance mode spectrum of the electrodes that is comparable to a longer structure. The manufacturing of the prototype by NTG, Gelnhausen, is currently in progress and is expected to be completed in Q3 2017.

References

- [1] P. Gerhard, L. Groening, K.-O. Voss, "In Situ Measurements of Mechanical Vibrations of a 4-Rod RFQ at GSI", Proc. of LINAC2014, Geneva, Switzerland, p. 553-555 (2014)
- [2] P. Gerhard, W. Barth, L. Dahl, W. Hartmann, G. Schreiber, W. Vinzenz, H. Vormann, "Experience with a 4-Rod CW Radio Frequency Quadrupole", Proc. of LINAC2012, Tel-Aviv, Israel, p. 825-827 (2012)
- [3] P. Gerhard, W. Barth, L. Dahl, A. Orzhekhovskaya, A. Schempp, K. Tinschert, W. Vinzenz, H. Vormann, M. Vossberg, S. Yaramyshev, "Commissioning of a New CW Radio Frequency Quadrupole at GSI", Proc. of IPAC'10, Kyoto, Japan, p. 741-743 (2010)

Upgrade measures for the UNILAC

*L. Groening^{*1}, X. Du¹, P. Gerhard¹, M. Heilmann¹, M.S. Kaiser¹, S. Mickat¹, A. Rubin¹, A. Seibel², H. Vormann¹, and C. Xiao¹*

¹GSI Helmholtzzentrum, 64291 Darmstadt, Germany; ²IAP, Goethe University Frankfurt, 60438 Frankfurt, Germany

In 2013 the UNILAC upgrade project [1] has been defined in order to prepare the machine to fulfil the requirements imposed by FAIR on beam quality and on operational reliability. The measures have been grouped into sub-projects and cover the full UNILAC from the installation of a dedicated uranium source up to the replacement of the post-stripper DTL. For each sub-project the target, required resources, schedule, risks, and boundaries have been summarized within a dedicated so-called Fact Sheet.

Handling and operation of uranium sources shall be localized at a dedicated source "terminal West" to be installed between the existing terminals "North" & "South" after the sub-project has been approved. The required fire protection concept for the new terminal is in preparation, now taking into account an overall concept for the ion source operation hall. The terminal will be followed by a short straight LEBT section [2]. This section ends with a new quadrupole quartet that is currently being installed at the entrance to the HSI-RFQ. The power supply for the new quadrupole quartet will be delivered soon.

The re-design of the HSI-RFQ electrodes has been started by A. Lombardi et al. from CERN within the overall CERN/GSI collaboration framework. The re-design aims for an improved envelope matching at the RFQ exit as well as for lowered electric surface fields during operation.

For the subsequent MEBT, providing for proper injection into the pre-stripper IH-DTL, a new design has been proposed already in 2014 [3]. It will notably increase the operational flexibility of the section by decoupling the transverse tuning from the longitudinal one. All components can be procured as soon as the funding has been approved. During the last years a new gaseous stripper cell has been developed. It aims for replacing the continuous nitrogen jet by a pulsed jet of hydrogen and for an increase of the target density. The new device provided for remarkable improvement of the stripping efficiency of about 68%. It additionally allows for pulse-to-pulse adaption of the jet parameters w.r.t. type of gas, pulse duration, and pressure. A detailed description of its development and performance is given in [4] and the references therein.

The aged post-stripper DTL will be replaced by a completely new DTL based on Alvarez-type cavities. This choice of technology has been made after a systematic and rigorous benchmarking procedure of several DTL-technologies finally commented and evaluated by external experts during a dedicated review [5]. Five independent cavities will provide for acceleration from 1.4 to

11.4 MeV/u. The rf-design includes improved drift tube shapes for maximum shunt impedance [6] as well as a novel scheme for field stabilization [7]. A 1:3 model cavity has been successfully tested [8] and a fully operational prototype cavity section is under preparation [9]. The new beam dynamics design [10] is optimized for delivery of intense uranium beams and will use pulsed quadrupoles inside the drift tubes, thus assuring optimized beam transport for each ion species being provided in quasi-parallel pulse-to-pulse switching mode. The cavities are separated by inter-tank sections, including a re-buncher each. These are required to provide smooth envelopes for provision of high quality beams. The bunchers will also be used to deliver beams of low energy spread for physics experiments at the Coulomb barrier. Extensive error studies w.r.t. machine errors as well as to fluctuations of the initial beam parameters have been performed. The upgrade of the DTL's rf-power alimentation system has been continued. A new 1.8 MW amplifier has been successfully tested at the manufacturer. In parallel the modularization of the alimentation system of the fourth cavity has well advanced [11].

All upgrade measures involving beam dynamics were modelled by front-to-end simulations based on measured beam parameters at the uranium source extraction gap. The fully upgraded UNILAC was modelled up to the entrance to the SIS18 [12]. These simulations provide the set of beam parameters to be achieved during stepwise commissioning of the upgraded UNILAC. The aged UHV control system needs to be modernized and first components have been ordered.

References

- [1] L. Groening et al., Proc. of 7th IPAC Conf. (2016).
- [2] C. Xiao et al., NIM A 788 p. 173 (2015).
- [3] H. Hähnel et al., Proc. of XXVII Linac Conf. (2014).
- [4] P. Scharrer et al., PRAB **20** 043503 (2017).
- [5] S. Mickat et al., this report.
- [6] X. Du et al., this report.
- [7] X. Du et al., PRAB **20** 032001 (2017).
- [8] A. Seibel et al., annual report of IAP, Univ. of Frankfurt (2016).
- [9] M. Heilmann et al., this report.
- [10] A. Rubin et al., this report.
- [11] B. Schlitt et al., this report.
- [12] C. Xiao et al., this report.

^{*}la.groening@gsi.de



ESR operation and development

C. Dimopoulou¹, R. Heß¹, M. Kelnhofer¹, C.M. Kleffner¹, S. Litvinov¹, F. Nolden¹, C. Peschke¹, N. Petridis¹, U. Popp¹, J. Roßbach¹, S. Sanjari¹, M. Steck^{*1}, and D. Winters¹

¹GSI Helmholtzzentrum, Darmstadt, Germany

In 2016, the experimental storage ring (ESR) has been operated from May to July for a period of about 5 weeks in total. A variety of interesting physics experiments, addressing different topics and using different new (FAIR-type) detector systems, could successfully be performed.

A new fast current transformer has been installed at the ESR, which allows for measurements of short ion bunches. The software for the ionization profile monitors (IPM), which were installed at the ESR a few years ago, has been updated and greatly improved. Therefore, it was possible to systematically perform measurements of the properties of bunched, electron-cooled ion beams.

From the 25th to the 29th of May, a uranium ion beam was offered for experiments at Cave A (HTA). The uranium ions ($^{238}\text{U}^{73+}$) extracted from the SIS18 were stripped by a carbon foil (12 mg/cm²), into the helium-like charge state ($^{238}\text{U}^{90+}$), and injected into the ESR at a kinetic energy of 192 MeV/u. After electron cooling, using the cooler as an electron target and exploiting the electron capture process, slow extraction of lithium-like ($^{238}\text{U}^{89+}$) ions towards Cave A could be performed. The beam could be delivered under good conditions, enabling precise spectroscopic measurements of the $2s_{1/2} - 2p_{3/2}$ transition in Li-like uranium, using the resonant coherent excitation process of relativistic ions in the *virtual photon field* of a thin silicon crystal. The lifetime of the stored beam was of the order of a few minutes.

From the 30th of May to the 7th of June, a uranium ion beam was offered for an atomic physics experiment at the internal target of the ESR. Li-like uranium ions ($^{238}\text{U}^{89+}$) were injected into the ESR at an energy of 76 MeV/u. After electron cooling, the ion beam was positioned such (by the *target bump*) that it had maximum spatial overlap with the gas jet. As a target, nitrogen (N₂) and xenon (Xe) gases were used. With the ion beam on target, the lifetime of the stored beam was about 1 minute. During the collisions between the Li-like ions and the target atoms, the ions can (non-)radiatively capture electrons into different states, or are excited, or lose an electron (ionization). Also two novel microcalorimeters have been successfully used to record the radiation emitted from the projectile-target interaction zone. The unique advantage of these microcalorimeters is that they can measure a broad X-ray energy spectrum with a high energy resolution. One microcalorimeter came from Heidelberg university, the other one from Giessen university. Finally, a VUV-spectrometer from Kassel university had been set up to look for specific radiation emitted from the target, during the collisions with the stored ions.

From the 13th to the 26th of June, a xenon ion beam was offered for an astrophysics experiment at the ESR. In a scattering process between projectile (Xe) and target (H₂), the projectile can capture a proton from hydrogen directly into the nucleus. The energy of the ions needs to be chosen low enough (Gamow window) to obtain stellar conditions. Special *in vacuo* particle detectors had previously been installed at the ESR to detect the charge-changed ions. The ($^{124}\text{Xe}^{54+}$) ions were injected into the ESR at an energy of 100 MeV/u. The experiments, using decelerated and electron-cooled ion beams and the internal target, could be performed at 30, 15, 8, 7, 6.7, 6, and 5.5 MeV/u. Under these conditions, the lifetime of the ion beams was of the order of only a few seconds. Especially the 5.5 MeV/u is very impressive, because it is the lowest energy thus far for an electron-cooled ion beam in the presence of a high-density target (density = $2 \times 10^{14} \text{ cm}^{-2}$).

From the 4th to the 6th of July, a Li-like carbon ion beam was offered for laser spectroscopy and laser cooling of stored and bunched ion beams in the ESR. The $^{12}\text{C}^{3+}$ ion beam was injected and stored at an energy of 122 MeV/u. The lifetime of the ion beam was of the order of a few tens of seconds, which was long enough for the laser spectroscopy measurements, but rather short for the laser cooling experiments. Stable ESR conditions were offered during the entire test beamtime. The laser systems have been developed by the TU-Darmstadt and the HZDR/TU Dresden and had a very good performance. The XUV detector, used for fluorescence measurements during laser spectroscopy, was installed and operated successfully by the University of Münster. The high-voltage of the electron cooler was recorded by a precision high-voltage divider (TU Darmstadt) and a high-precision digital voltmeter, which were installed inside the Faraday cage of the electron cooler.

From the 7th to the 11th of July, a bare carbon ion beam was offered for tests with CRYRING@ESR [1]. The goal was to extract and transport the ions, at very low energies, through the very long beamline towards CRYRING@ESR. The $^{12}\text{C}^{6+}$ ions were first electron-cooled inside the ESR, then decelerated, again electron-cooled, and finally extracted from the ESR at two energies, 6 MeV/u and 18 MeV/u, in order to compare results. This endeavor was a great success, and the arrival of ions at the first fluorescent screen inside the ring could be demonstrated.

References

- [1] F. Herfurth *et al.*, GSI scientific report 2016.

* m.steck@gsi.de

Progress with the barrier bucket system for ESR *

D. Domont-Yankulova^{†1}, J. Harzheim¹, K. Groß¹, H. Klingbeil^{1,2}, and M. Frey²

¹TU Darmstadt, Germany; ²GSI, Darmstadt, Germany

Introduction

A new barrier bucket system is designed for the ESR storage ring at GSI. It will be used to precompress or to stack the beam longitudinally [1]. The core part of the system are the RF cavities where single-sine voltage pulses with defined amplitude \hat{U}_{BB} and repetition frequency $1/T_{rev}$ have to be generated. These RF pulses are used as potential barriers. To compress the beam one of the pulses is shifted in time (see figure 1).

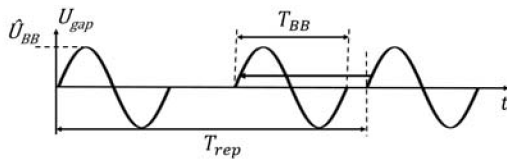


Figure 1: Shifting of the single sine pulses

To achieve pulses with the required high quality a model of the pulse generation system is essential. So in the last year we put efforts into the improvement of a PSpice cavity model and into the nonlinear behavior of the amplifier for high voltage amplitudes.

PSpice model of the cavity

In last year's scientific report [2], we presented a method how to systematically generate an equivalent circuit model for broadband cavities from ring core measurement data. The transfer function of these models showed good agreement with measurements, but the measured impedance still differed from simulation results. In order to improve the model, the coupling windings (see figure 2) were modeled more accurately by a two conductor transmission line and an ideal coupler. The transmission line parameters were estimated analytically from winding geometry and ring core properties.

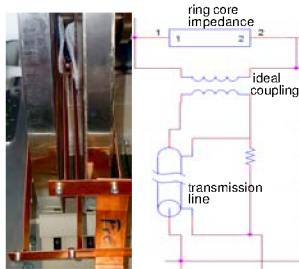


Figure 2: Cavity windings and PSpice model

* Work supported by GSI

[†] D.Domont-Yankulova@gsi.de

The refined modeling decreased the difference between measurement and simulation of the impedance (see figure 3) and improved the accuracy of the simulated transfer function even further.

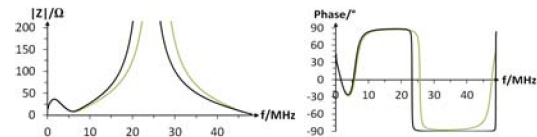


Figure 3: Impedance, comparison between measurement and simulation.

Operation in the nonlinear range

As pointed out in the last GSI annual report [3] it is possible to generate single sine gap signals of high quality in a wide voltage range (up to 550 V) by using linear methods. However at high amplitudes, nonlinear effects can be observed and have to be taken into account. Arguing from the setup structure, it is reasonable to assume a static nonlinearity located right after the amplifier entrance. In a first attempt, we determined the nonlinearity by measuring the peak of the gap voltage for sine input signals of different amplitude and smoothened the obtained characteristic by a 4th order polynomial. Figure 4 shows that taking the nonlinearity of the amplifier into account improves the quality of the output signal. Now, amplitudes of up to 760 V can be generated with the same setup and good signal quality.

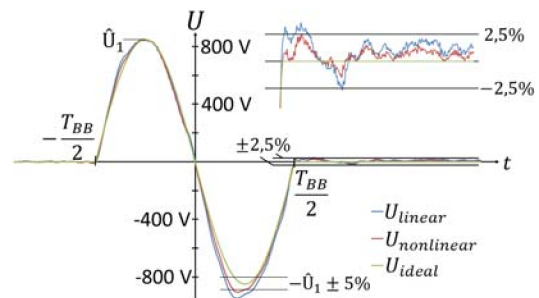


Figure 4: Linear and nonlinear predistortion for $\hat{U} = 820$ V

References

- [1] M. Steck, et al., "Demonstration of Longitudinal Stacking in the ESR with Barrier Buckets and Stochastic Cooling", Proc. Workshop on Beam Cooling and Related Topics (COOL'11), Alushta, Ukraine, 2011
- [2] J. Harzheim, et al., "Modeling of broadband cavities in PSpice", GSI SCIENTIFIC REPORT 2015
- [3] M. Frey, et al., "Status of the Barrier-Bucket system for the ESR", GSI SCIENTIFIC REPORT 2015

The status of the CRYRING@ESR project - First Turn*

F. Herfurth^{†1}, M. Lestinsky¹, Z. Andelkovic¹, R. Bär¹, A. Bräuning-Demian¹, S. Litvinov¹, O. Dolinskii¹, W. Enders¹, M. Engström¹, S. Fedotova¹, B. Franzke¹, W. Geithner¹, O. Gorda¹, A. Källberg², N. Kotovskiy¹, A. Reiter¹, A. Simonsson², T. Sieber¹, J. Sjöholm², M. Steck¹, Th. Stöhlker^{1,3}, G. Vorobjev¹, and the CRYRING@ESR team¹

¹GSI, Darmstadt, Germany; ²MSL, Stockholm University, Stockholm, Sweden; ³HJ, Jena, Germany

The low energy storage ring LSR [1] will provide highly charged ions and antiprotons at low energy for two collaborations at FAIR, SPARC and FLAIR. Those collaborations intend to perform precision experiments pursuing atomic and nuclear physics questions [2] whose preparation is well on track [3]. The LSR is a Swedish in-kind contribution to the FAIR facility in Darmstadt.

The LSR is the low energy storage ring CRYRING modernized and adapted to the additional needs for injection and ejection of antiprotons and highly charged ions at about 10 MeV/nucleon. CRYRING has been operated at the Manne Siegbahn Laboratory in Stockholm until 2010, was dismantled in 2012 and transported to GSI in the first months of 2013. At GSI it is being installed behind the ESR, as proposed and described in detail in 2012 by a swedish-german working group [4].

CRYRING can decelerate, cool, and store heavy, highly charged ions and antiprotons injected at about 10 MeV/nucleon down to a few 100 keV/nucleon. It provides a high performance electron cooler and a straight section for flexible experiment installations as for instance a gas jet target. It is equipped with its own injector and ion source, to allow for standalone commissioning.

The ring hardware and all infrastructure is in place and the local injector has been commissioned [5]. In summer the transfer of ions from the ESR to CRYRING@ESR has been successfully commissioned online. For this, a bunch of C^{6+} ions, decelerated and cooled in the ESR to 6 MeV/nucleon (corresponding to a beam rigidity $B\rho \approx 0.7$ Tm), was transported to the first diagnostic station in CRYRING@ESR - a fluorescent screen. The modified transport beam line from ESR to Cave B (where CRYRING@ESR has been set up) has been fully operational, including the newly built magnetic septum for fast injection. The successful transport of a beam with such low rigidity is promising when it comes to the robustness of this transfer line even at settings well below the design rigidity. The planned regular transport rigidity is about 1.4 Tm, slightly higher than the one originally designed for protons injected into the LSR. The injection kicker in CRYRING@ESR was upgraded to be able to handle this beam rigidity and tested in summer successfully offline at the vendors factory.

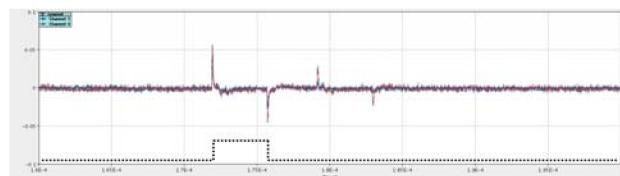


Figure 1: Raw signal as recorded from beam position monitors, i.e. capacitive pickups, that show twice the passage of the injected single bunch. Plotted is the signal amplitude in arbitrary units versus time. The injected ion bunch shape is sketched in the lower part of the plot.

A dedicated off-line commissioning beam time, using the local injector and H_2^+ ions, was used to achieve the first turn. The pressure in the ring was not lower than a few times 10^{-8} mbar because the system has not been baked yet and hence the NEG pumps were not activated. A short ion bunch of about $4 \mu s$ has been created with the beam chopper in the injector in order to have a bunch shorter than one turn at the injection energy of 300 keV/nucleon.

With a peak intensity of up to $2 \mu A$ the bunch was injected into the ring and after optimising the injection line elements, signals on the installed first turn diagnostics, two fluorescent screens and three faraday cups, have been observed.

The signal displayed in fig. 1 only shows the quickly changing components of the passing ion beam. To be more sensitive to the complete signal the capacitive coupling to the preamplifiers has been adapted. Results of the change will make it easier to detect also weak signals during the upcoming beam tests.

References

- [1] H. Danared, et al. (2011) "LSR - Low-energy Storage Ring, Technical design report", MSL, Stockholm University, v 1.3.
- [2] M. Lestinsky, et al. (2015), "CRYRING@ESR: Present Status and Future Research", Phys. Scr. T166, 014075 (2015).
- [3] M. Lestinsky, et al. (2016), "Progress of experimental systems for CRYRING@ESR", GSI annual scientific report 2016.
- [4] M. Lestinsky, et al. (2012) "CRYRING@ESR: A study group report", GSI, Darmstadt,
- [5] W. Geithner, et al. (2017), "Status and outlook of the CRYRING@ESR project", 2017, Hyperfine Interact., 238, 13

* Work supported by GSI/HI Jena/FAIR@GSI PSP code:1.3.4.2/The SPARC collaboration/Uni Krakov/KVI Groningen

[†] F.Herfurth@gsi.de

Installation progress of the electron cooling system at CRYRING

J. Roßbach¹, C. Dimopoulou¹, R. Heß¹, M. Bräscher¹, M. Kelnhofer¹, and J. Krieg¹

¹GSI, Darmstadt, Germany

Activities regarding the CRYRING electron cooler concentrated on completing the media supplies (electrical power, cooling water, cryogenics). The demineralized water cooling system for the normal conducting magnets was equipped with a pressure reducer in order to match the specifications for the cooler magnets operation. Some repairs had to be done to several leaks which occurred during the commissioning of the cooling system. Water hoses had also to be replaced because they caused an electrical short-circuit to earth and disabled the commissioning of the magnet power supplies. The electron cooler uses in total three coldheads/cryopumps, they are driven by two helium cryocompressors. The latter need special cooling water (softened water, not demineralized) which has been provided by a separate cooling system.

The liquid helium transfer line was delivered and installed in May 2016, thus completing the helium supply system. The commissioning of the superconducting gun solenoid took place at the end of 2016. A first successful test with magnetic field strengths up to 3 T was carried out, as required for the cooler operation. (Fig. 1)



Figure 1: Magnetic field of 3 T and corresponding electric current (51 A) in the superconducting magnet during the test. The cold magnet kept its field in persistence mode i.e. after the current power supply was switched off.

Two cryopumps, on the gun and collector side, are essential to improve the vacuum pressure for the cooler operation. They had to be refurbished on site: service of the coldheads, exchange of the absorber inside the cryocompressor, purging of the whole helium system. A similar service was necessary for the coldhead of the solenoid cryostat: Its cooling power was not sufficient to keep the thermal shield within the cryostat cold. This led to fast liquid helium loss (evaporation) out of the bath of the superconducting coil. After the service the coldhead performs appropriately.

The 3.5 kV high voltage power supply of the collector broke down; due to its age and poor current resolution (3 A) it was replaced by a new device allowing the measurement of the electron beam current reaching the collector with high resolution (16 bits, 0-200 mA). Several other

high voltage power supplies were refurbished. To protect the cooler against unsecure operating conditions a hardware interlock system was designed and implemented. It protects the cooler against bad vacuum pressure, loss of cooling water in the collector, loss of the accelerating high voltage, loss of the magnetic field in the gun superconducting solenoid.

The pickups installed within the cooler main solenoid have been successfully tested with ion beam. Furthermore, due to space restrictions, making it difficult to attach and detach them, the RF cables connected to the pickup vacuum feedthroughs were substituted by bakeable ones. For future laser experiments, the scrapers used in Sweden were reinstalled at their ports within the toroid chambers at the gun and collector side.

Regarding the cooler vacuum system, its assembly was completed. Vacuum measurement gauges as well as a high-voltage feedthroughs had to be changed. The electron gun itself was equipped with a new cathode and was installed into the gun vacuum chamber. The cryopumps at gun and collector were mounted. First bake out of the vacuum system took place in April 2017.

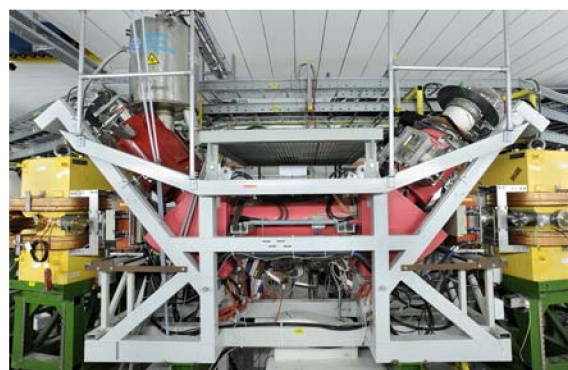


Figure 2: Recent view of the complete electron cooler in the CRYRING cave.

The application program for the remote control and operation of the electron cooler was further developed. All electron cooler magnet and high-voltage power supplies were created as a FESA model, tested and released.

Standalone commissioning of the electron cooler with its electron beam is scheduled for May 2017. Cooler operation with ion beam will follow later in 2017.

Beam instrumentation of the RFQ injector at CRYRING

A. Reiter, F. Herfurth, T. Sieber, G. Vorobjev

GSI, Darmstadt, Germany

for the Dept. of Beam Instrumentation and the CRYRING collaboration

Introduction

This contribution reports on the beam instrumentation in the RFQ injector and the experiences gained throughout the linac commissioning in 2016. It completes an earlier report on this topic [1] and provides an update on modifications to beam line and instrumentation.

Ion Source Beam Line

The injector together with the positions of the beam instrumentation is shown in Fig. 1. Continuous beams of light, singly-charged ions of 10 keV/u, mainly H_2^+ , have been extracted from a MINIS ion source and cut to pulses of several 100 μs by a chopper. To increase filament life-time and current, the ion source will be modified for pulsed operation. An isolated iris or AC transformer (ACT) will be added to the current measurement system to monitor the source stability. The plasma around the filament is monitored by a special camera that looks upstream from the 0° port of the dipole chamber into the ion source.

Before and after the 90° spectrometer dipole, current and distribution of the primary beam can be measured with a Faraday cup (FC) or a scintillating screen (SCR) [2]. The combination of multi-channel plate and 25 mm phosphor P43 has turned out to be too sensitive. More robust and larger 50 mm Chromox screens with an anti-static wire mesh will be their replacement.

The beam line, apart from the dipole, is composed of electrostatic elements. Together with beam instrumentation devices they are supplied from a common high voltage (HV) system with FESA software and graphical user interface (GUI). All HV mainframes are network devices with TCP/IP control. An industrial PC hosts a base FESA class which provides access to all HV channels, e.g. to a quadrupole FESA class that converts a field gradient calculated by the ion optics model to HV set values of the four quadrupole electrodes.

At the RFQ entrance a segmented iris, consisting of four isolated plates, aids the optimisation of the beam injection into the linac. The plate currents are fed to a charge-to-frequency converter, and the output pulses are registered in a dedicated VME scaler. A GUI displays left-right and top-bottom asymmetry together with a list of scaler values.

Radio-Frequency Quadrupole Linac

The 108.5 MHz RFQ linac accelerates ions of $q/A > 0.36$ to about 300 keV/u. Beam currents of 1.5 μA for H_2^+ have

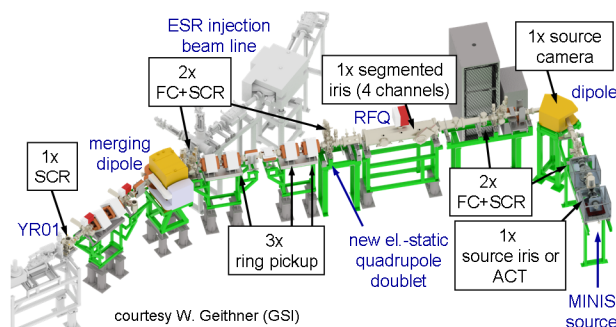


Figure 1: Overview of RFQ injector and diagnostics elements. The total length is ~ 10 m. ESR beam line and first ring section YR01 are shown in grey colour.

been routinely achieved with a transmission of 50%. With pulsed source operation the new target value is 10 μA . Behind the RFQ, a quadrupole doublet replaces the debuncher, which - due to its small diameter - caused significant losses and lead to spurious effects in the time-of-flight energy measurements. The bunch monitoring system analyses pairs of signals selected from three pickups or the RFQ tank. A FESA application controls signal gain and readout of a 5 GSa/s digital oscilloscope. The analysis is described in [3]. The GUI displays signals traces and trends of pickup voltages, energy and tank power. The energy of ~ 295 keV/u is in good agreement with previous measurements and is reached at the expected power of $P=12$ kW following the empirical rule $P=3 \cdot (A/q)^2$ kW for this RFQ. The FESA application can be ported to the HITRAP decelerator and serve during linac commissioning, e.g. of the 1.4 MeV/u continuous-wave demonstrator cavity in 2017.

At the RFQ exit and before the merging dipole the same FC/SCR detector combinations as in the ion source beam line are available. Both detectors are mounted in a compact chamber on a common stepper motor drive. Close to the injection septum, a bakeable Chromox screen on a pneumatic drive acts as injection monitor. The new PLC system has been recently completed with FESA class and GUI. All infrastructure systems (HV, stepper motors, and pneumatic drives) can be fully integrated into the control system.

References

- [1] A. Reiter et al., GSI Scientific Report 2013
- [2] B. Walasek-Höhne et al., TUPD062, IBIC 2014, Stanford, USA
- [3] A. Reiter et al., MOPD35, DIPAC 2011, Hamburg, Germany

A detection system for laser spectroscopy experiments at CRYRING *

A. Buß^{†1}, Z. Andelkovic³, V. Hannen¹, C. Huhmann¹, W. Nörtershäuser², D. Thomas¹, and Ch. Weinheimer¹

¹WWU Münster, Institut für Kernphysik, Wilhelm-Klemm-Str. 9, 48161 Münster;

²Technische Universität Darmstadt, Institut für Kernphysik, Schlossgartenstraße 9, 64289 Darmstadt;

³GSI Helmholtzzentrum für Schwerionenforschung GmbH, Planckstraße 1, 64291 Darmstadt

The low energy storage ring CRYRING is being set up as the first storage ring of the upcoming accelerator facility FAIR at GSI. In order to enable laser spectroscopy experiments with stored ions, a fluorescence detection system is currently being developed at the Institut für Kernphysik in Münster. It will be set up in section 7 of CRYRING. The detector is designed to measure in a broad wavelength regime between 250 nm to 900 nm.

Several ions of interest have transitions in this wavelength regime. For instance Mg^+ (at 280 nm) and Ba^+ (at 313 nm). The latter is a relevant candidate for studying laser induced dielectronic recombination (LIDR).

So far, simulations of the optical system have been performed in order to optimize the detection efficiency for laser-induced fluorescence photons, while - at the same time - reducing the detection probability for background photons.

Geant4 Monte Carlo simulations show [1], that a geometry with a focusing ellipse is a well performing design in order to enhance fluorescence detection, while suppressing detection of background photons uniformly generated in the detector's sensitive volume. The working principle of this geometry is shown in figure 1 in the projection on the ion beam axis. Next to it, the reflectivity of the ellipse's surface material MIRO3[®] is shown.

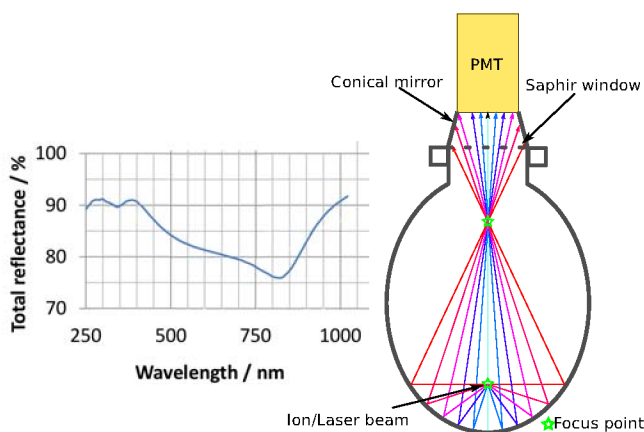


Figure 1: Left: reflectivity of MIRO3[®], right: focusing ellipse principle

Both, the ion and the laser beam are passing through the lower focus point of the ellipse. The laser induced fluorescence photons are emitted nearly isotropically (as ions

in CRYRING are only slightly relativistic). The geometry of the ellipse reflects photons that hit the elliptical surface through the upper focus point. Eventually, they can be measured by one of three PMTs on the top of the setup. Two sets of PMTs will be procured, one for the UV and one for the long wavelength range ($\gtrsim 900$ nm). Depending on the wavelength of the observed transition, the PMTs can be interchanged easily, as they are located outside of the vacuum. For the infrared-sensitive PMTs, a cooling housing is needed in order to reduce background from thermal noise.

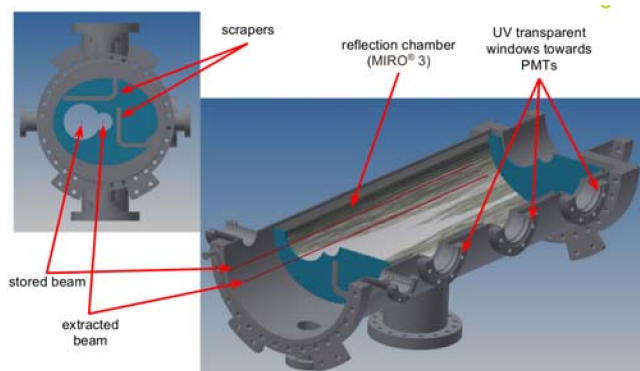


Figure 2: Cross section of the vacuum enclosure and mirror chamber of the detection system.

The estimated collection efficiency of the geometry amounts to 19.5% for beam photons and 2.3% for background photons at a wavelength of 350 nm. This number contains the wavelength-dependent reflectivity and transmission coefficients of the used materials. Not included in the number is the quantum efficiency of the PMTs.

The design of the detector is currently being finalized. First components have been procured.

References

- [1] D. Thomas, bachelor thesis, Institut für Kernphysik Münster, 2016

* Supported by BMBF under contract number 05P15PMFAA

[†] axel.buss@uni-muenster.de

Precision high voltage divider for the electron cooler at CRYRING *

D. Winzen^{†1}, I. Denesjuk¹, V. Hannen¹, W. Nörtershäuser², H.-W. Ortjohann¹, O. Rest¹, and Ch. Weinheimer¹

¹Institut für Kernphysik, Uni Münster; ²Institut für Kernphysik, TU Darmstadt

The low energy storage ring CRYRING@ESR is currently being commissioned as the first storage ring for FAIR phase-0 at GSI. CRYRING features an electron cooler in order to cool stored ions and thus achieve a low momentum spread of the beam. To determine the velocity of the ions a precise knowledge of the acceleration voltage of the electron cooler is essential.

Therefore we construct a high-precision divider for voltages up to 35 kV which will be similar to the ultrahigh-precision voltage dividers which have been constructed in Münster in cooperation with PTB for use at the KATRIN experiment [1, 2]. The precision of the divider will be in the low ppm range and will allow for measurement uncertainties in the $< 10^{-5}$ region.

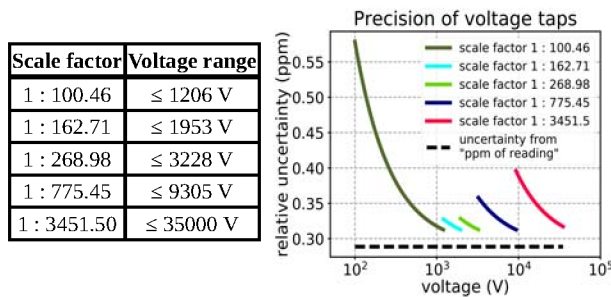


Figure 1: Left: Scale factors of voltage taps. Right: Precision of voltage taps for 8.5 digit DVM resolution (Keysight 3458a).

High-voltage dividers usually consist of many high voltage resistors R_i connected in series to allow for the requested maximum voltage. The available Vishay VHA518-11 resistors [3] to be installed in the high-voltage divider have been characterized and tested for stability. The output voltage U_{out} is measured using a high-precision digital voltmeter over the low voltage resistance R_{LV} . A voltage divider is characterized by the scale factor M of its voltage tap (1):

$$M = \frac{U_{in}}{U_{out}} = \frac{\sum_i R_i + R_{LV}}{R_{LV}} \quad (1)$$

The scale factor describes the factor between input and output voltage and has to be matched to the high-voltage range of interest and the most sensitive range of the applied digital voltmeter (< 20 V for commercially available precision 8.5 digit voltmeters). For measurement ranges

from 0.1 kV up to 35 kV the high voltage divider will provide different scale factors by implementing different low voltage outputs (figure 1).

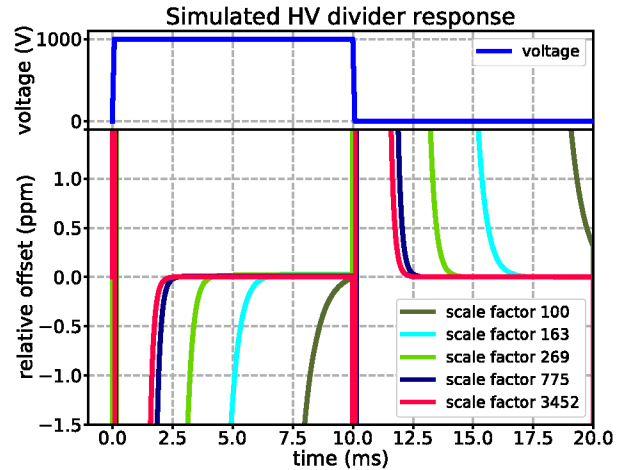


Figure 2: Top: Application of 1000 V detuning voltage with 12V/ μ s ramping speed. Bottom: High-voltage divider response relative to ideal value (3 ppm window).

Besides static electron cooler voltage measurements, a detuning of the electron cooler voltage for approx. 10 ms is necessary for electron-ion merged-beam experiments [4]. Therefore the high-voltage divider response times have been investigated using LTspiceXVII. In figure 2 the response of the different voltage taps to a 1000 V offset as provided by a Kepco Bop 1000m are shown. For scale factors > 100 the voltage signal stabilizes in the 10 ms window allowing for DVM integration times of approx. 4-7 ms corresponding to 6.5 digit precision measurements.

The design of the divider has been finalized. Construction is currently ongoing and aimed to be finished in summer 2017. Subsequently calibration measurements will be conducted using a new absolute calibration method developed in Münster. This calibration will also be available for use at GSI to calibrate the divider on a regular basis.

References

- [1] T. Thümmel *et al.*, New J. Phys. 11 (2009) 103007
- [2] S. Bauer *et al.*, JINST 8 (2013) P10026
- [3] Vishay, <http://www.vishaypg.com/docs/63006/hmetlab.pdf>
- [4] Andelkovic Z *et al.*, Technical Design Report: Experimental Instrumentation of CRYRING@ESR FAIR Facility for Antiproton and Ion Research

* Supported by BMBF under contract number 05P15PMFAA

[†] d.winzen@uni-muenster.de

